



**Calhoun: The NPS Institutional Archive**  
**DSpace Repository**

---

Theses and Dissertations

1. Thesis and Dissertation Collection, all items

---

1968-05

## A dual mode roll stabilization system.

Richmond, Frederick James

Massachusetts Institute of Technology

---

<http://hdl.handle.net/10945/40086>

---

This publication is a work of the U.S. Government as defined in Title 17, United States Code, Section 101. Copyright protection is not available for this work in the United States.

*Downloaded from NPS Archive: Calhoun*



Calhoun is the Naval Postgraduate School's public access digital repository for research materials and institutional publications created by the NPS community. Calhoun is named for Professor of Mathematics Guy K. Calhoun, NPS's first appointed -- and published -- scholarly author.

**Dudley Knox Library / Naval Postgraduate School**  
**411 Dyer Road / 1 University Circle**  
**Monterey, California USA 93943**

<http://www.nps.edu/library>

NPS ARCHIVE  
1968  
RICHMOND, F.

A DUAL MODE ROLL  
STABILIZATION SYSTEM

Author: Frederick James Richmond

Thesis Supervisor: Prof. George C. Newton

Date Submitted: May 17, 1968

Thesis  
R395

A DUAL MODE ROLL  
STABILIZATION SYSTEM

by

FREDERICK JAMES RICHMOND  
B.E.E., AUBURN UNIVERSITY

(1961)

SUBMITTED TO THE DEPARTMENT OF NAVAL ARCHITECTURE AND MARINE  
ENGINEERING IN PARTIAL FULFILLMENT OF THE REQUIREMENTS FOR  
THE MASTER OF SCIENCE DEGREE IN ELECTRICAL ENGINEERING  
AND THE PROFESSIONAL DEGREE, NAVAL ENGINEER

at the

MASSACHUSETTS INSTITUTE OF TECHNOLOGY

May, 1968

Signature of Author . . . . . *Frederick J. Richmond* . . . . .

Department of Naval Architecture and  
Marine Engineering, May 17, 1968

Certified by . . . . . *George C. Newton* . . . . .

George C. Newton, Professor of Electrical  
Engineering, Thesis Supervisor

Certified by . . . . . *Martin A. Abkowitz* . . . . .

Martin Aaron Abkowitz, Professor of Naval  
Architecture, Reader for the Department

Accepted by . . . . .

Chairman, Departmental Committee on  
Graduate Students



LIBRARY  
NAVAL POSTGRADUATE SCHOOL  
MONTEREY, CALIF. 93943-5101

A DUAL MODE ROLL

DUDLEY KNOX LIBRARY  
NAVAL POSTGRADUATE SCHOOL  
MONTEREY, CA 93943-5101

STABILIZATION SYSTEM

by

FREDERICK JAMES RICHMOND

ABSTRACT

Submitted to the Department of Naval Architecture and Marine Engineering on May 17, 1968, in partial fulfillment of the requirements for the Master of Science Degree in Electrical Engineering and the Professional Degree, Naval Engineer.

The Deep Submergence Rescue Vehicle is being built with an activated roll stabilization system. The effectiveness of this system is limited by pump saturation. This investigation is concerned with improving the roll stabilization of the DSRV through the use of a passive tank stabilizer. A mathematical model for the tank system is developed and adapted to the DSRV model. The passive system is extended to include two modes of operation, each representing a separate tank frequency, which may be selected by the operation of a valve. The passive system and the dual mode system are simulated on an analog computer to determine their response to transient disturbances.

The results show that a passive stabilizer of reasonable design could improve the roll stabilization of the vehicle. Furthermore, it is concluded that stabilization of transient disturbances can be improved by dual mode operation if a tank frequency at least three times greater than the natural frequency of the vehicle can be obtained for one of the two tank modes.

Thesis Supervisor: George C. Newton  
Title: Professor of Electrical Engineering

NOMENCLATURE

A) Variables and Forcing Functions

$x, y, z$	Coordinate directions, vehicle body reference frame: x forward, y to starboard, z down
$u, v, w$	Fluid velocities, inertial reference
$\phi$	Roll angle, positive to starboard
$\theta$	Pitch angle, positive bow up
$\psi$	Yaw angle, positive bow to starboard
$S$	Curvilinear fluid displacement along centerline of tank
$K$	Roll-producing moment applied to vehicle
$K_f$	Moment applied to tank fluid
$K_v$	Moment applied to vehicle resulting from tank fluid motion

B) Parameters Related to Tank Geometry

$A(S)$	Tank cross-sectional area as a function of $S$
$A$	Pipe cross-sectional area
$A_T$	Side tank cross-sectional area
$\alpha_{Ave}$	Proportionality constant relating force to fluid velocity
$\beta$	Tank fluid angle
$d$	Perpendicular distance between roll axis and any point on tank centerline
$D_F$	Energy dissipated in fluid flow
$D_p$	Damping term: a coefficient which includes effects of flow loss
$\sqrt{g/L}$	Natural frequency of fluid motion in tank system
$\gamma$	Angle between $r$ and $d$ .
$I'_x$	Vehicle moment of inertia about roll axis modified by removal of passive system fluid

$J_T$	Tank moment of inertia about roll axis
$K_1$	A parameter reflecting conservation of fluid angular momentum
$L$	Tank effective length
$\ell$	Pipe length
$M^2$	Tank curvature constant
$M_{Ty}$	Tank moment about pitch axis
$n$	Number of connecting pipes
$R$	Side tank lever arm
$r$	Radius to any point on tank centerline
$T_f$	Fluid kinetic energy
$V_f$	Fluid potential energy
$V_T$	Tank volume
$v_T$	Total fluid velocity
$w'$	Vehicle weight modified by removal of passive system fluid weight

C) Other Notation Used

$g$	Acceleration due to gravity
$h$	Differential height between two fluid levels
$H_f$	Head loss in feet
$t$	Time in seconds

# LIST OF FIGURES

<u>No.</u>	<u>Title</u>	<u>Page</u>
I	Velocity Components of a Fluid Particle Within a U-Tube Tank . . . . .	6
II	Basic Tank Geometry . . . . .	17
III	Case I, $g/L$ Versus $D_p$ . . . . .	20
IV	Case II, $g/L$ Versus $D_p$ . . . . .	21
V	Passive System Simulation Diagram . . . . .	25
VI	Responses to Initial Velocities . . . . .	27
VII	Case I and Case II Responses to Initial Heel Angle . . .	28
VIII	Case II Responses to Ramp Moments. . . . .	29
IX	Response to Periodic Disturbances . . . . .	30
X	Effect of Pipe Roughness . . . . .	31
XI	Comparison between Existing System and the Passive System	32
XII	Valve Simulation Diagram . . . . .	34
XIII	Mode Switching Arrangement . . . . .	40
XIV	Valve Timing and Mode Control . . . . .	40
XV	Comparison between Dual and Single Mode Operation. . . .	41
XVI	Comparison between Dual and Single Mode Operation . . .	42
XVII	Comparison between Dual and Single Mode Operation . . .	43
XVIII	Dual Mode Response Showing Effect of $k_1$ . . . . .	44



## TABLE OF CONTENTS

	<u>Page</u>
Title Page . . . . .	i
Abstract . . . . .	ii
Nomenclature . . . . .	iii
List of Figures . . . . .	v
Chapter I    General Discussion of Roll Stabilization . . . . .	1
Chapter II   Modeling the Passive Tank System . . . . .	5
Chapter III   Selection of Tank Geometry and Parameters . . . . .	15
Chapter IV   System Simulation . . . . .	23
Chapter V   Discussion of Results and Conclusions . . . . .	36
Appendix I   The DSRV Model . . . . .	45
Appendix II   Parameter Calculations . . . . .	50
References . . . . .	56



## CHAPTER I

### GENERAL DISCUSSION OF ROLL STABILIZATION

#### Introduction

Roll stabilization of ships at sea has been an area of engineering interest for many years. Historically, the first recorded attempt to build a functional roll-stabilization system occurred during the latter years of the 19th century. Since that time there has been a steady technical effort directed at improving roll-stabilization techniques and equipment. Roll-stabilization has been recognized as a problem not unlike conventional servo mechanism problems.<sup>1</sup> Accordingly, more recent technical advances within the discipline of automatic control have been used successfully to overcome many of the control problems which plagued early systems.

Currently, the most widely used roll-stabilization systems are generally of the fin type or the moving fluid type. However, moving solid weights and gyroscopes have also been used in the past as the major element of stabilization systems. The use of fin type stabilizers is somewhat restricted, in that their effectiveness decreases rapidly with ship speed. However, fin stabilization systems have been used successfully for many years aboard ships which operate primarily at or near their designed speed. Moving fluid systems (unlike fins) provide reliable stabilization at all speeds. These systems are grouped into one of two categories. A passive system is one which depends upon gravity and inertial effects alone for the transfer of fluid mass. An activated system employs some type of pumping device to force the transfer of fluid mass within the system.

In either the active or the passive system, the principle of operation is the same. Energy is imparted to the ship system as a result of wind

2

and wave action or by other transient forces and moments such as those produced by ship control surfaces. The added energy is partially transferred to the stabilization system's fluid mass. The fluid system is a conservative system, except for the energy dissipated due to flow losses. The resulting fluid motion develops forces and moments which oppose the ship motion and thus produce the stabilizing effect. The effectiveness of an anti-roll system is therefore dependent on the system's ability to transfer energy to the fluid, the fluid-to-ship motion phase relationship, and the energy dissipation characteristics of the fluid flow. Energy transfer to the fluid and the flow losses are primarily a function of the tank geometry. The phase relationship between fluid and ship motion depends primarily on tank geometry for passive systems. For active systems, the pump and control system responses, as well as the tank geometry, determine the phase relationship.

In general, activated systems are capable of greater roll reduction than are passive systems under similar conditions. However, as in most physical systems, a penalty must be paid for higher performance. In activated roll-stabilization systems, the penalty appears in the form of the weight and power requirements of the system's pump.

#### The DSVR and Roll Stabilization

The Deep Submergence Rescue Vehicle (DSVR) is being designed with control capability in six degrees of freedom. The synthesis and simulation of this system has been reported in the literature.<sup>4</sup> Of primary interest in this investigation is the proposed DSVR list-control system, which, under cruising conditions (or hovering with zero list), would



effectively be an activated roll-stabilization system. List control in the proposed DSVR system is to be effected by pumping mercury between a set of three tanks. Appendix I illustrates the system model.

Pertinent to the subject of roll stabilization of the DSVR are some of the physical characteristics of the vehicle. Basically, the DSVR will have a body-of-revolution hull form with few significant appendages. The transverse metacenter is very near the axis of symmetry of the body of revolution, and as a result, the natural damping of the vehicle is practically negligible. The lack of natural damping places a heavy burden on the list control system, because the system must then compensate for any and all disturbances in the roll mode.

The DSVR, like many other deep submersible vehicles, is power and weight-limited. For this reason there is a physical limitation as to the size and capacity of the pump used in the list control system. Therefore, in operation, the system is subject to pump saturation which severely degrades the vehicle stabilization in the roll mode. Furthermore, because of nearly continuous pump operation, the power requirements of this system become an important factor in overall vehicle endurance.

This investigation will be concerned with the adaptation of a passive roll stabilization system which will complement the existing DSVR roll-control system. A tank system similar to a conventional U-tube stabilizer will be considered initially.<sup>2</sup> This system will be extended to employ a valve arrangement which may be controlled in such a manner as to utilize the effects of gravity and inertia to enhance the transfer of fluid mass within the system. The purpose of the valve is to increase the rate of



mass transfer and thus counteract the effects of pump saturation as experienced by the existing DSVR roll-control system. The investigation will use as a basis the DSVR geometry and vehicle model as reported in reference four and outlined in Appendix I. The modified model which will be assumed will not alter the exterior characteristics of the existing model.

MODELING THE PASSIVE TANK SYSTEM

Assumptions

It is assumed that a second tank system is designed and added to the existing DSRV vehicle. The existing roll-control system is left intact except that a portion of the existing mercury will be used in the second system. It is also assumed for the purposes of this investigation that the total vehicle mass is unaltered by the addition of the passive system. The tank system will be assumed similar in design to the U-tube type shown in Fig. I.

The Mathematical Model

The general equations describing the fluid motion are developed using a Lagrangian approach. Three basic expressions are required to define the total energy of the fluid mass. Thus, expressions for the kinetic energy, the potential energy, and the energy dissipated due to fluid motion are required. Throughout the following development, translational velocity of the vehicle and fluid in the x-direction is neglected.

To define the kinetic energy of the fluid, an expression for its velocity is required. A fluid particle has the following velocities in the y- and z- directions (see Fig. I):

$$v = \dot{y} + \dot{\psi} X_{\psi} \cos \psi + \dot{S} \frac{A_T}{A(S)} \sin (\beta - \phi + \gamma) - \dot{\phi} r \sin (\beta - \phi) \quad (2.1)$$

$$w = \dot{z} - \dot{\theta} X_{\theta} \cos \theta + \dot{S} \frac{A_T}{A(S)} \cos (\beta - \phi + \gamma) - \dot{\phi} r \cos (\beta - \phi) \quad (2.2)$$

Since kinetic energy depends on the square of total velocity ( $v_T^2 = v^2 + w^2$ ), an expression for  $v_T^2$  is required.

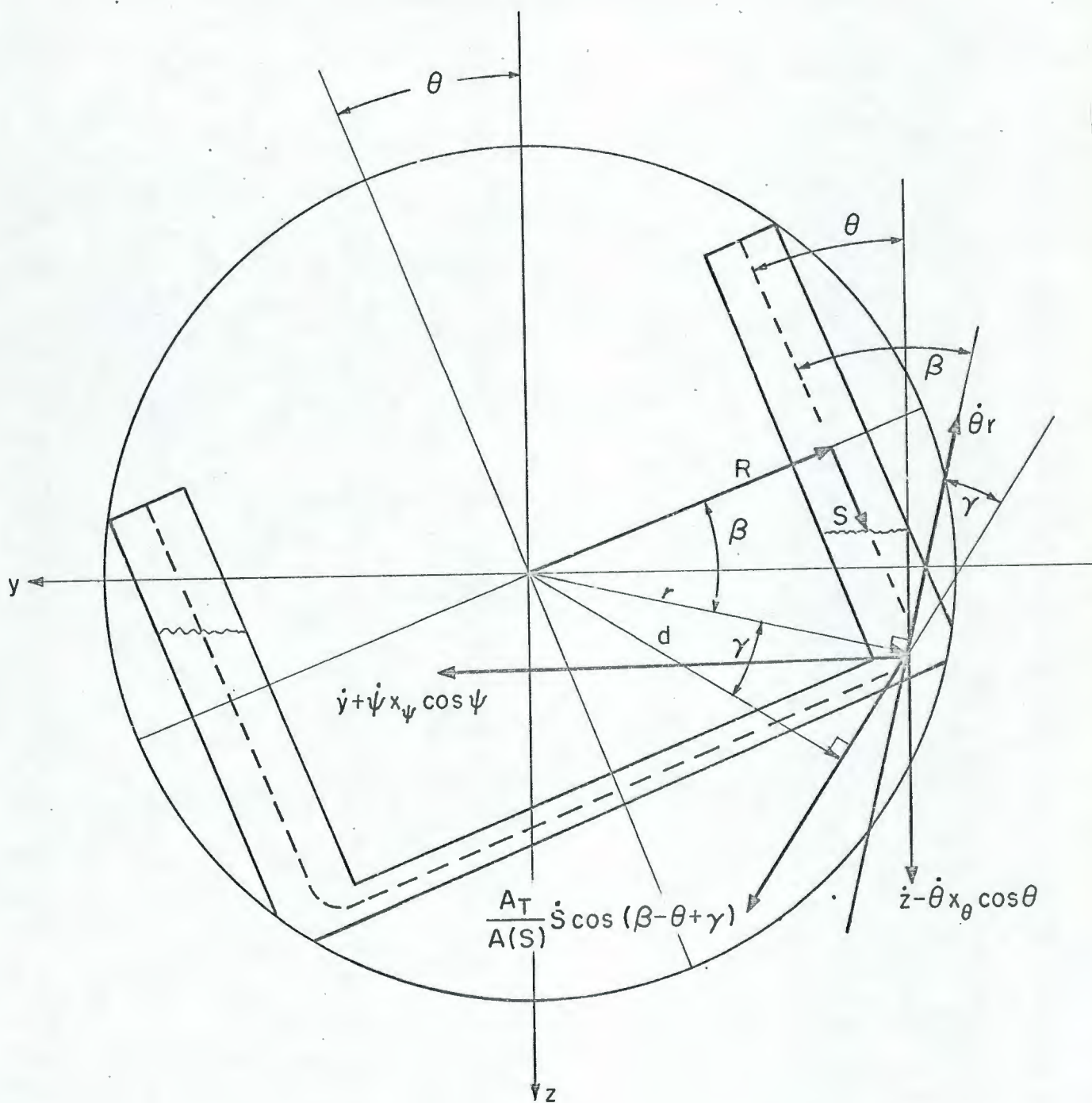


Figure I

Velocity Components of a Fluid Particle Within a U-Tube Tank



$$\begin{aligned}
v_T^2 = & \dot{z}^2 - 2\dot{z}\dot{x}_\theta \dot{\theta} \cos \theta + \dot{\theta}^2 x_\theta^2 \cos^2 \theta + 2\dot{z} \dot{S} \frac{A_T}{A(S)} \cos (\beta - \phi + \gamma) \\
& - 2\dot{z}\dot{\phi} r \cos (\beta - \phi) - 2\dot{\theta} x_\theta \dot{S} \frac{A_T}{A(S)} \cos (\beta - \phi + \gamma) \cos (\theta) \\
& + 2\dot{\theta} x_\theta \dot{\phi} r \cos \theta \cos (\beta - \phi) + \dot{S}^2 \left[ \frac{A_T}{A(S)} \right]^2 \cos^2 (\beta - \phi + \gamma) \\
& - 2 \left[ \frac{A_T}{A(S)} \right] \dot{S} \dot{\phi} r \cos (\beta - \phi) \cos (\beta - \phi + \gamma) \\
& + \dot{\phi}^2 r^2 \cos^2 (\beta - \phi) + \dot{y}^2 + \dot{\psi}^2 x_\psi^2 \cos^2 \psi \\
& + \dot{S}^2 \left[ \frac{A_T}{A(S)} \right]^2 \sin^2 (\beta - \phi + \gamma) + \dot{\phi}^2 r^2 \sin^2 (\beta - \phi) \\
& + 2\dot{y}\dot{\psi} x_\psi \cos (\psi) + 2\dot{y}\dot{S} \left[ \frac{A_T}{A(S)} \right] \sin (\beta - \phi + \gamma) \\
& - 2\dot{y}\dot{\phi} r \sin (\beta - \phi) + 2\dot{\psi} x_\psi \dot{S} \left[ \frac{A_T}{A(S)} \right] \cos \psi \sin (\beta - \phi + \gamma) \\
& - 2\dot{\psi} x_\psi \dot{\phi} r \cos \psi \sin (\beta - \phi) \\
& - 2\dot{S}\dot{\phi} r \left[ \frac{A_T}{A(S)} \right] \sin (\beta - \phi + \gamma) \sin (\beta - \phi)
\end{aligned} \tag{2.3}$$

Making the approximation that fluid velocity is constant at any cross-section within the tank system, the kinetic energy of such a cross-section may be expressed as follows:

$$dT_f = \left( \frac{v_T^2}{2} \right) dm$$

where  $dm = \rho A(S) ds$

Therefore, total fluid kinetic energy may be expressed as:

$$T_f = \int \frac{\rho A(S) v_T^2}{2} ds \tag{2.4}$$

Substituting Equation 2.3 and noting that the tank volume ( $V_T$ ) is  $\int A(S)ds$  produces the following expression:

$$\begin{aligned}
 T_f = & \frac{\rho}{2} \{ \dot{z}^2 - 2\dot{z}\dot{X}_\theta \cos \theta + \dot{\theta}^2 X_\theta^2 \cos^2 \theta + \dot{y}^2 + \dot{\psi}^2 X_\psi^2 \cos^2 \psi + 2\dot{y}\dot{\psi} X_\psi \cos \psi \} V_T \\
 & - \rho \dot{\phi} (\dot{y} + \dot{\psi} X_\psi \cos \psi) \int A(S) r \sin(\beta - \phi) ds \\
 & - \rho \dot{\phi} (\dot{z} - \dot{\theta} X_\theta \cos \theta) \int A(S) r \cos(\beta - \phi) ds \\
 & + \rho \dot{S} A_T (\dot{y} + \dot{\psi} X_\psi \cos \psi) \int \sin(\beta - \phi + \gamma) ds \\
 & + \rho \dot{S} A_T (\dot{z} - \dot{\theta} X_\theta \cos \theta) \int \cos(\beta - \phi + \gamma) ds \\
 & + \frac{\rho A_T \dot{S}^2}{2} \int \left( A_T / A(S) \right) ds + \frac{\dot{\phi}^2}{2} \int \rho r^2 A(S) ds + \rho A_T \dot{S} \dot{\phi} \int r \cos \gamma ds
 \end{aligned} \tag{2.5}$$

This expression may be simplified by using the approximations  $\sin \phi = \phi$  and  $\cos \phi = 1$ . These approximations are valid under conditions of small roll angles which are to be expected in a stabilized vehicle. The first integral in Equation 2.5 thus becomes:

$$\int A(S) r \sin(\beta - \phi) ds = \int A(S) r \sin \beta ds + \phi \int A(S) r \cos \beta ds$$

The first integral on the right above is recognized as the tank moment ( $M_{Ty}$ ) about the pitch axis. The second integral is, by inspection, zero because of the tank symmetry. Therefore:

$$\int A(S) r \sin \beta ds = M_{Ty} \tag{2.6}$$

Similarly:

$$\int A(S) r \cos(\beta - \phi) ds = \int A(S) r \cos \beta ds - \phi \int A(S) r \sin \beta ds = -\phi M_{Ty} \tag{2.7}$$

The third and fourth integrals in expression 2.5 are seen (see Fig. 1) to reduce as follows:

$$\begin{aligned} \int \cos(\beta - \phi + \gamma) ds &= \int \cos(\beta + \gamma) ds - \phi \int \sin(\beta + \gamma) ds \\ &= 0 - \phi 2R \end{aligned} \quad 2.8a$$

$$\begin{aligned} \int \sin(\beta - \phi + \gamma) ds &= \int \sin(\beta + \gamma) ds + \phi \int \cos(\beta + \gamma) ds \\ &= 2R + 0 \end{aligned} \quad 2.8b$$

where R is the tank radius.

Investigation of the three remaining integrals in expression 2.5 reveals that these represent constants that are unique to the chosen geometry of the tank system. The following definitions are made:

$$\frac{1}{2} \int \left( \frac{A_T}{A(S)} \right) ds \triangleq L \quad (\text{Effective length}) \quad 2.9$$

$$\int r \cos \gamma ds \triangleq M^2 \quad (\text{Curvature constant}) \quad 2.10$$

$$\int \rho r^2 A(S) ds \triangleq J_T \quad (\text{Tank moment of inertia}) \quad 2.11$$

Substituting equations 2.6 through 2.11 into Equation 2.5 yields the kinetic energy expression:

$$\begin{aligned} T_f = \frac{\rho}{2} & (\dot{z}^2 - 2\dot{z}\dot{X}_\theta \cos \theta + \dot{\theta}^2 X_\theta^2 \cos^2 \theta + \dot{y}^2 + \dot{\psi}^2 X_\psi^2 \cos^2 \psi + 2\dot{y}\dot{\psi} X_\psi \cos \psi) V_T \\ & + (\dot{y} + \dot{\psi} X_\psi \cos \psi) (+ \rho \dot{S} A_T 2R - \rho \dot{\phi} \dot{M}_{Ty}) \\ & - (\dot{z} - \dot{\theta} X_\theta \cos \theta) (\phi 2R \rho \dot{S} A_T + \rho \dot{\phi} \dot{\phi} \dot{M}_{Ty}) \\ & + \rho A_T \dot{S}^2 L + \frac{J_T^2}{2} \dot{\phi}^2 - \rho A_T \dot{S} \dot{\phi} M^2. \end{aligned} \quad 2.12$$

The expression for potential energy may be considered to have three components each of which may be calculated separately. With the tanks blocked ( $S = 0$ ), the potential energy of the fluid due to roll is given by the expression:



$$V_{f_1} = \rho g \left\{ \int A(S)r \sin \beta \, ds - \int A(S)r \sin \beta \cos \phi \, ds \right\}$$

Letting  $\cos \phi = 1 - \frac{\phi^2}{2}$  this equation reduces to:

$$V_{f_1} = \rho g \frac{\phi^2}{2} \int A(S)r \sin \beta \, ds = \frac{\rho g \phi^2}{2} M_{Ty} \quad 2.13$$

The potential energy contribution due to pitch (tanks blocked) is:

$$V_{f_2} = \frac{1}{2} \rho g V_T X_\theta \sin^2 \theta.$$

Letting  $\sin \theta = \theta$  this becomes:

$$V_{f_2} = \frac{1}{2} \rho g V_T X_\theta \theta^2. \quad 2.14$$

The potential energy contribution due to fluid motion in the tanks is given by:

$$V_{f_3} = \rho g A_T S(S \cos \phi - 2R \sin \phi)$$

As previously stated, the total potential energy is the sum of the three components.

$$\begin{aligned} V_f &= V_{f_1} + V_{f_2} + V_{f_3} \\ V_f &= \frac{\rho g}{2} \phi^2 M_{Ty} + \frac{1}{2} \rho g V_T X_\theta \theta^2 + \rho g A_T S(S - 2R\phi) \end{aligned} \quad 2.15$$

The dissipative energy expression will be postulated to be a function of the cube of the fluid velocity relative to the tank system.

$$D_f = \frac{D_o}{3} \dot{S}^3 \quad 2.16$$

The function  $D_o$  is not yet specified.

The generalized coordinates which are of principal interest in this development are  $\phi$  and  $S$ <sup>6</sup>. The two Lagrange equations of interest are, therefore:

$$\frac{d}{dt} \left( \frac{\partial T_f}{\partial \dot{\phi}} \right) - \frac{\partial T_f}{\partial \phi} + \frac{\partial V_f}{\partial \phi} + \frac{\partial D_f}{\partial \phi} = K_f \quad 2.17$$

$$\frac{d}{dt} \left( \frac{\partial T_f}{\partial \dot{S}} \right) - \frac{\partial T_f}{\partial S} + \frac{\partial V_f}{\partial S} + \frac{\partial D_f}{\partial S} = 0 \quad 2.18$$

It should be noted that Equation 2.17 is a moment equation and that  $K_f$  represents the moment (in the  $\phi$  direction) applied to the fluid of the tank system. Equation 2.18 is a force equation representing the force applied to the fluid in the  $S$  direction.

Using  $T_f$ ,  $V_f$ , and  $D_f$  as defined by Equations 2.12, 1.15 and 2.16, respectively, in Equations 2.17 and 2.18 produces the following two basic system equations:

$$J_T \ddot{\phi} + \rho g M_{Ty} \phi - \rho A_T M^2 \ddot{S} - 2\rho g R A_T S + (\dot{z} - \dot{\theta} X_{\theta} \cos \theta) 2R \rho A_T \dot{S} - \rho M_{Ty} (\ddot{y} + \ddot{\psi} X_{\psi} \cos \psi + \ddot{\phi} z - \dot{\phi} \dot{\theta} X_{\theta} \cos \theta) = K_f \quad 2.19$$

$$2\rho A_T L \ddot{S} + D_o \dot{S}^2 + 2\rho g A_T S - 2\rho g R A_T \phi - \rho A_T M^2 \ddot{\phi} + 2\rho A_T R (\ddot{y} + \ddot{\psi} X_{\psi} \cos \psi - \ddot{z} \dot{\phi} + \dot{\phi} \ddot{\theta} X_{\theta} \cos \theta - \ddot{\phi} z + \dot{\phi} \ddot{\theta} X_{\theta} \cos \theta) = 0 \quad 2.20$$

These equations will be simplified by considering the terms containing the variables  $\dot{z}$ ,  $\ddot{z}$ ,  $\ddot{y}$ ,  $\dot{\theta}$ ,  $\ddot{\theta}$  and  $\ddot{\psi}$  to be disturbance inputs. The value of any one of these variables would be small during any reasonable vehicle maneuver and a first-order approximation would be to assume that all terms



containing the product of two variables are negligibly small. However, since the  $D_O \dot{S}^2$  term in Equation 2.20 will be retained as the tank damping term, it would be inconsistent to set all product terms to zero. Alternatively, it will simply be assumed that the disturbance inputs may be individually set to zero so that attention may be focused on the relationship between vehicle roll and fluid displacement. In addition to the simplifying assumptions, Equation 2.19 is altered by noting that any moment applied to the tank fluid must be opposed by an equal moment acting on the tank. Thus, Equations 2.19 and 2.20 become, respectively:

$$J_T \ddot{\phi} + \rho g M_{Ty} \phi - \rho A_T M^2 \ddot{S} - 2\rho g R A_T S = -K_V \quad 2.21$$

$$2 \rho A_T L \ddot{S} + D_O \dot{S}^2 + 2\rho g A_T S - A_T M^2 \ddot{\phi} - 2\rho g R A_T \phi = 0 \quad 2.22$$

The forcing term in Equation 2.21 ( $K_V$ ) is the moment applied to the vehicle as a result of fluid motion within the tank system.

#### Adapting the Tank Model to the DSRV

The simplified equation of motion in roll for the basic DSRV (see Appendix I) is:

$$(I_x - K_p) \ddot{\phi} = -w z_g \phi + K_s + K_{p|u|} |\dot{u}| \dot{\phi} \quad 2.23$$

The coefficients of Equation 2.23 must be modified to reflect the change in the amount of mercury assigned to the basic vehicle model. The effected terms are  $I_x$  and  $w$  which will be designated  $I'_x$  and  $w'$  to denote the modification. The total moment ( $K_S$ ) applied to the vehicle is considered to be the sum of two components

$$K_S = K_V + K \quad 2.24$$

Combining equations 2.22 and 2.23 by using 2.24 yields the basic moment equation for the vehicle modified by the addition of the passive tank



system.

$$\begin{aligned}
 & (I'_x - K_p + J_T) \ddot{\phi} - K_p |u| |u| \dot{\phi} + (w'_z + \rho g M_{Ty}) \phi \\
 & - \rho A_T M^2 \ddot{S} - 2 \rho g R A_T S = K
 \end{aligned} \tag{2.25}$$

Equation 2.25 together with Equation 2.22 defines the relationship between ship roll and fluid displacement.

Recall that Eq. 2.22 is a force equation where each term represents a force acting on the fluid. The term  $D_o \dot{S}^2$  represents the friction force due to fluid flow. Since this force always opposes fluid motion, it can be approximated by the following expression:

$$D_o \dot{S}^2 \approx K_{Dp} |\dot{S}| \dot{S} \tag{2.26}$$

The approximate proportionality constant  $K_{Dp}$  is evaluated in Appendix II.

Substituting Eq. 2.26 in Eq. 2.22 and rearranging yields:

$$\ddot{S} = g/L \left\{ - \frac{K_{Dp}}{2 \rho g A_T} |\dot{S}| \dot{S} - S + \frac{M^2}{2g} \ddot{\phi} + R\phi \right\} \tag{2.27}$$

Similarly, Equation 2.25 becomes:

$$\begin{aligned}
 \ddot{\phi} = & \left( \frac{1}{I'_x - K_p + J_T} \right) \left\{ + K_p |u| |u| \dot{\phi} - (w'_z + \rho g M_{Ty}) \phi + \rho A_T M^2 \ddot{S} + \right. \\
 & \left. 2 \rho g R A_T S + K \right\}
 \end{aligned}$$

or

$$\ddot{\phi} = + A_1 \dot{\phi} - A_2 \phi + A_3 \ddot{S} + A_4 S + A_5 K \tag{2.28}$$

where:

$$A_5 = 1 / (I'_x - K_p + J_T) \tag{2.29}$$

$$A_1 = K_p |u| |u| A_5 \tag{2.30}$$

$$A_2 = (w'_z + \rho g M_{Ty}) A_5 \tag{2.31}$$

$$A_3 = \rho A_T M^2 A_5 \tag{2.32}$$

$$A_4 = 2 \rho g R A_T A_5$$

2.33

Equations 2.27 and 2.28 are in a form suitable for simulation on an analog computer. Furthermore, in this form the significance of the various tank parameters is readily seen. The coefficient  $g/L$  in Eq. 2.27 will be defined as the square of the tank natural frequency (as indeed it would be, if the equation were linear). Note also that, from Equations 2.25 and 2.31, the coefficient  $A_2$  is the squared natural frequency of the vehicle modified by the tank system. The coefficient  $K_{DF}/2 g A_T$  will be referred to as the tank damping term. Tank frequency and damping are discussed in the next chapter in connection with the selection of the tank geometry.



SELECTION OF TANK GEOMETRY AND PARAMETERS

As previously stated, the passive tank system design is to be compatible with existing DSRV external geometry. Some of the basic design considerations are fairly self-evident. For example, to result in maximum effectiveness, the system should utilize the maximum ship beam, and locating the tanks at or near the ship's yaw axis will minimize the inter-coupling effects between fluid motion and yaw. It is assumed that the tank can be located on a transverse plane that includes the yaw axis. It is also assumed that no portion of the system will be more than 3.5 feet from the vehicle's longitudinal axis. The latter constraint is required to keep the tank system within the exterior skin of the vehicle.

A basic parameter in tank selection is the volume of fluid the system is to use. Previous experience has indicated two fundamental design points for tank selection.<sup>5</sup> The first such point is that a total fluid weight of between 1/2% and 1-1/4% of total ship displacement is sufficient to produce effective roll stabilization if the tanks are properly arranged. Design point two is that for a steady list of 1°, the tank static moment should be at least 12% of the moment to heel 1°.

To satisfy the first point, it is assumed that 1.66 cubic feet of mercury (equal in weight to 1% of total vehicle displacement) will be used in the passive system. This, by assumption, reduces the amount of mercury in the existing DSVR roll-control system by 50%. Allowing for 100% fluid transfer under extreme conditions, each side tank volume must then be at least 1.66 cu. ft. A tank area of 0.6 square feet was selected, on the basis of being a compromise between reduced tank lever arm and the



overall tank length. The tank is assumed to be round in cross-section, with a curved vertical axis so as to conform to the geometry of the DSVR. Figure II illustrates the geometry. The small tank area and the assumed free surface have a negligible effect on vehicle static stability. This assumed tank arrangement results in a static tank moment for  $1^\circ$  of heel equal to about 25% of the moment to heel  $1^\circ$ , and is thus well within the guidelines of design point two.

The selection of the geometry for the cross-connecting portion of the tank system becomes somewhat more involved. Since this portion of the system constitutes a major portion of the tank's overall length, the shape and size of the cross-connect directly affects the tank parameters  $M_{Ty}$ ,  $L$ ,  $M^2$  and  $J_T$ . In addition, the tank damping term is primarily a function of the geometry of this section. This latter point results from the fact that the damping term is dependent upon fluid friction which, in turn, is dependent on surface area exposed to the fluid flow.

In selection of the cross-connect geometry, four factors were considered. For the side tank arrangement shown in Fig. II, a maximum (case 1) and a minimum (case 2) overall pipe length were selected for investigation. Six pipe cross-sectional areas were considered, which correspond to inside diameters of 0.08, 0.09, 0.10, 0.11, 0.12 and 0.13 feet. These values were selected because, in the author's judgment, they represented realistic values for such an application. Another factor considered was the total number of connecting pipes. Calculations were made for the use of one through eight connecting pipes; however, pipe diameters were not mixed for any single calculation. The last factor considered in the tank parameter calculations was

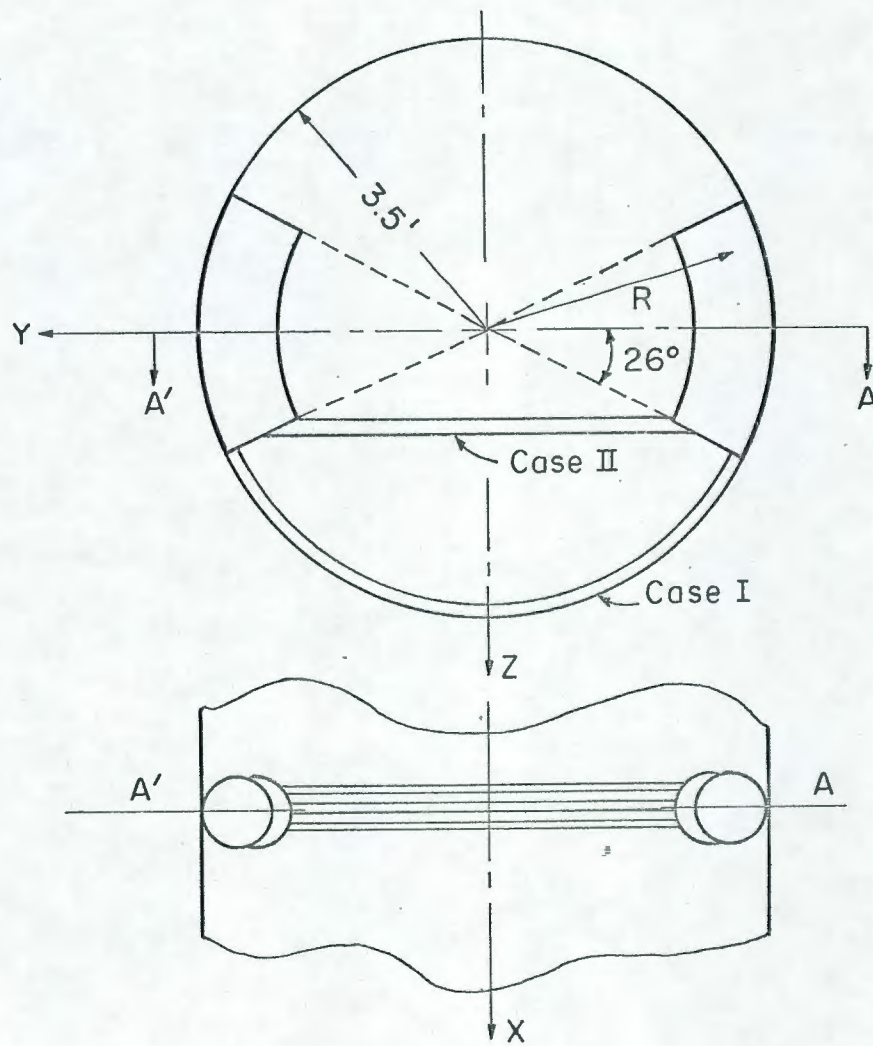


Figure II

Basic Tank Geometry



pipe roughness. The basis for all damping term calculations was a Moody diagram (see reference 7, page 15) which is a plot of friction factor ( $f$ ) versus Reynolds number. The curves given for smooth pipe flow and fully rough flow were used in these calculations to illustrate the range of the expected damping term.

The first step in the calculations was to solve equations 2.6, 2.9 - 2.11 for  $M_{Ty}$ ,  $L$ ,  $M^2$  and  $J_T$  respectively. This was done for both case 1 and case 2 with  $n$  (the number of pipes) and  $A_p$  (the pipe cross-sectional area) as variables. These calculations and results are documented in Appendix II.

The calculation of the damping term is based on a theoretical maximum fluid velocity for static conditions of maximum heel. For transient fluid flow from a tank under the conditions of no friction, no body forces and tank diameter much larger than pipe diameter, the velocity in the pipe is given by the expression:<sup>7</sup>

$$V = \sqrt{2gh} \tanh(t\sqrt{2gh/2l}) \quad 3.1$$

The maximum velocity for the assumed geometry under conditions of 30° of heel is therefore 16 ft/sec. under ideal flow conditions. This figure is used as a maximum value in calculating the damping term. It should be noted that from Eq. 3.1 about four seconds, or about 35% of the DSVR's natural period of roll, is required to reach the maximum velocity.

The force exerted on the fluid flow due to friction was calculated by using the equation:

$$\text{Pounds force} = \rho g A_p H_f = \rho A_p \{1.5 + f(l/d)\} V^2/2 \quad 3.2$$

In the above expression,  $l/d$  is the pipe length to diameter ratio,  $f$  is the friction factor obtained from the Moody chart, and the 1.5 represents



an approximation of the entrance and exit losses of the flow. The results of Equation 3.2 (for velocities between 1.0 and 16.0 feet/sec) were averaged to determine an approximate proportionality constant. The result is the following:  $F = \alpha_{Ave} V^2$ . Note that from Eq. 2:27 the term  $K_{Dp} |\dot{S}| S$  is the force term related to the fluid velocity in the side tanks. Since the tank velocity and the pipe velocity are related by the ratio of the respective areas and the number of pipes, the force term may be written as:

$$K_{Dp} S |\dot{S}| = n \alpha_{Ave} V^2 = n \alpha_{Ave} \left( \frac{A_T}{n A_P} \right)^2 V^2 \quad 3.3$$

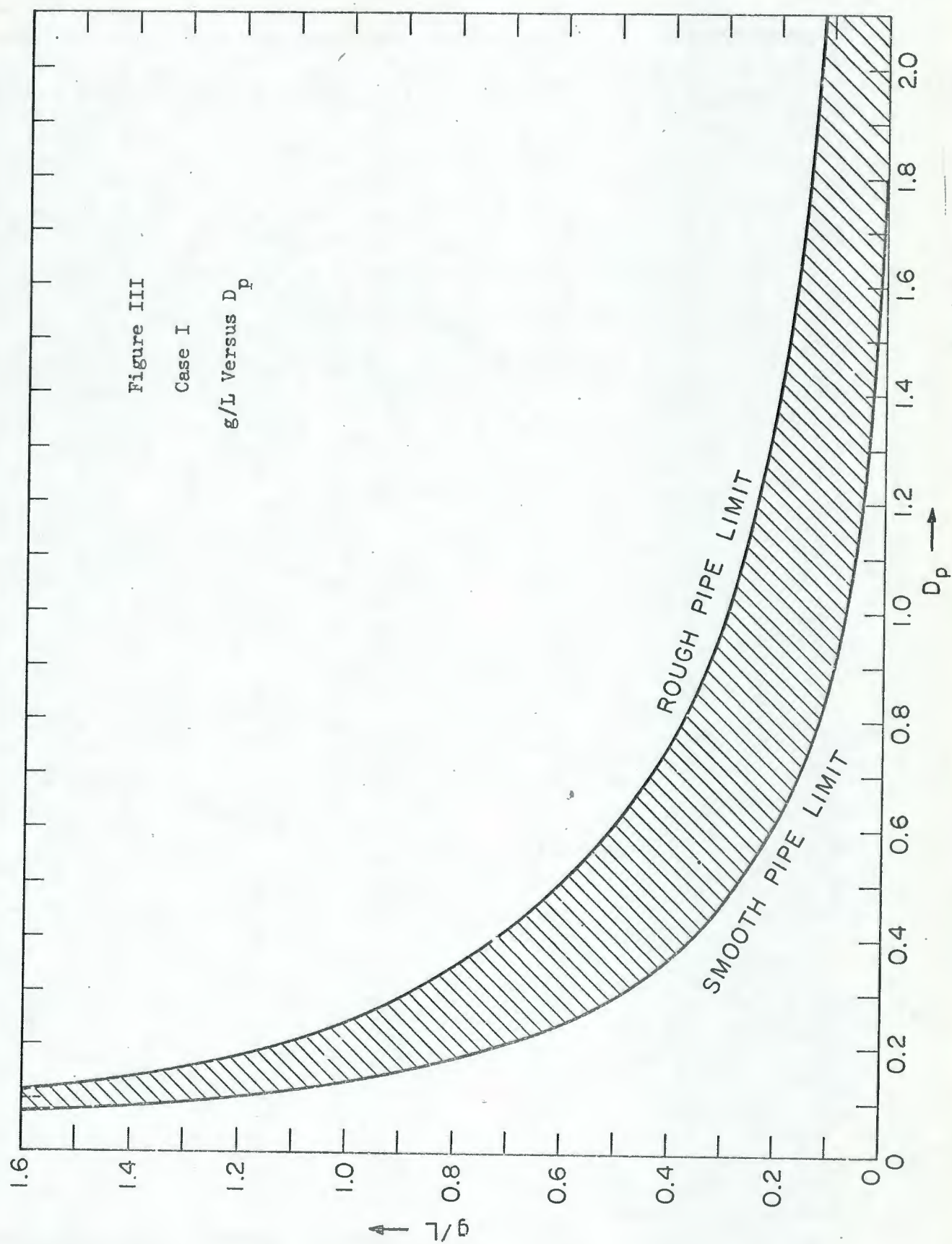
From the above it is clear that:

$$K_{Dp} = \frac{\alpha_{Ave}}{n} \left( \frac{A_T}{A_P} \right)^2 \quad 3.4$$

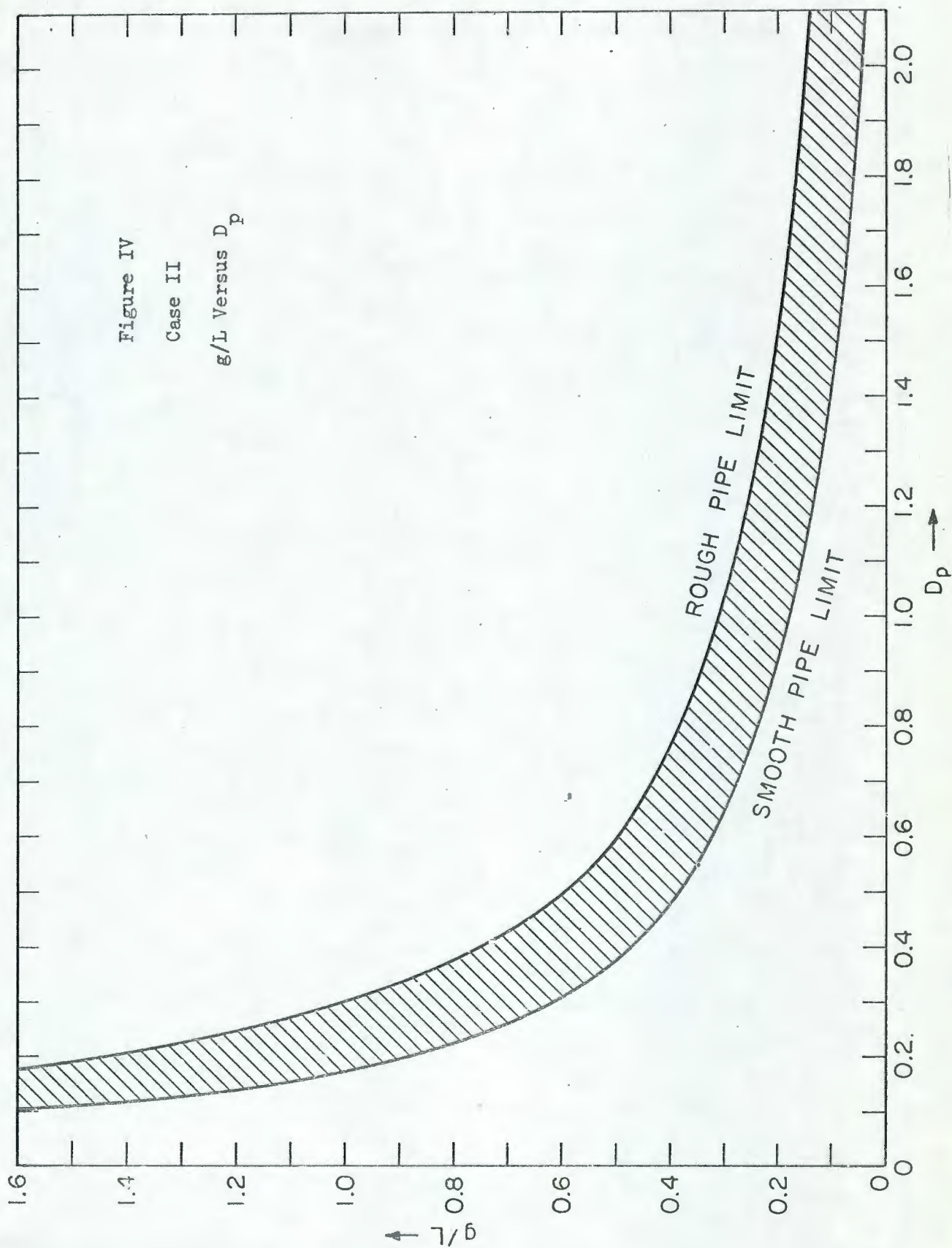
The relationship between the square of tank frequency and the tank damping term are shown for case 1 and case 2 in Figures III and IV respectively.

The two geometry cases considered were selected because it was felt they would establish realistic end points. Case two, because of the minimum effective tank length (single pipe), produced the minimum tank period. Therefore, maximum mass-transfer rates are to be expected from this geometry. No attempt was made to optimize tank geometry.

In a practical system, tank tuning could be accomplished by varying the amount of fluid in the system, by selective switching of various cross-connect length/number of pipes, or by using valves to throttle the flow in the cross-connect pipes. Yet another possibility for tank tuning is to have a secondary fluid on top of the tank fluid (for a mercury system, oil









could be used as the secondary fluid.) Tuning could then be accomplished by throttling the return flow of the secondary fluid. However, any of these possibilities could be used only to decrease the tank frequency from the maximum possible from the case II geometry.

The calculations for pipe damping should be recognized as approximate rather than absolute values. The damping term results represent the range of values which could be expected from a physical system. However, in an actual system design, more accurate results could be obtained from physical model tests.

## CHAPTER IV

SYSTEM SIMULATIONThe Passive System

The first simulation\* attempts of this system were conducted under conditions which were calculated to show the effectiveness of the conventional passive system. Equations 2.27 and 2.28, which represent the passive system, were used as the basis of this simulation.

The system coefficients as defined by Equations 2.29 through 2.33 were evaluated on the basis of the previously selected tank geometry. The coefficient  $A_1$  has a very weak dependence on the tank moment of inertia, since  $J_T$  is less than 1% of the vehicle's moment of inertia. Therefore this coefficient was taken as a constant ( $1.62 \times 10^{-5} \text{ Slug}^{-1} \text{ ft}^{-2}$ ) throughout the simulation (see Appendix I for the numerical evaluation). The coefficient  $A_1$  as defined by Eq. 2.30 represents a damping term which is dependent on vehicle motion in the horizontal plane. A worst case was assumed where the vehicle would be in the hover mode ( $u=0$ ) and therefore  $A_1$  would go to zero. The coefficient  $A_2$  as defined by Eq. 2.31 was evaluated and found to be rather insensitive to variations of the tank parameter  $M_{Ty}$ . As noted in Chapter two, this coefficient represents the natural frequency (squared) of the vehicle modified by the tank system. The evaluation indicates that within the two assumed geometry cases, the natural frequency of the vehicle is approximately a constant. The values used for  $A_2$  are:

---

\* The analog computer simulation of this system was carried out on a GPS model 200T analog computer. The simulated system's output was recorded on a dual channel, model 60, Sanborn Strip Recorder. Both pieces of equipment are part of the facilities of the Electronic Systems Laboratory.



$$\text{Case I: } A_2 = .324 \text{ Sec}^{-2} \quad 4.1$$

$$\text{Case II: } A_2 = .319 \text{ Sec}^{-2}$$

as defined by Eq. 2.32,  $A_3$  has a strong dependence on the tank curvature constant. The values used for this coefficient are:

$$\text{Case I: } A_3 = .0089 \text{ Feet}^{-1}$$

$$\text{Case II: } A_3 = .0041 \text{ Feet}^{-1}$$

The coefficient  $A_4$  which is defined by Eq. 2.33, is dependent upon the side tank geometry. Since this was assumed constant for both Case I and Case II, the coefficient  $A_4$  is a constant. The value used is:

$$A_4 = 0.0507 (\text{Feet/Sec}^2)^{-1} \quad 4.3$$

The coefficients of Eq. 2.27 are all dependent on tank geometry. The tank frequency (squared) and the tank damping term are tabulated in Tables II and IV respectively. The other two coefficients,  $M^2/2g$  and  $R$ , are self-explanatory.

Initial simulation of the single mode passive system was conducted to study the effectiveness of the passive tank system. It was assumed that the vehicle roll-control system was inoperative, so that the full effect of the passive system could be observed. The basic system computer-simulation diagram is shown in Fig. V. Scale factors have not been included for simplicity. Initial conditions simulating transient disturbances of heel ( $\phi$ ) and rolling ( $\dot{\phi}$ ) were applied to the vehicle model and the resulting damping effect recorded. The system model was also subjected to a series of ramp and sine wave inputs, simulating a variety of disturbance



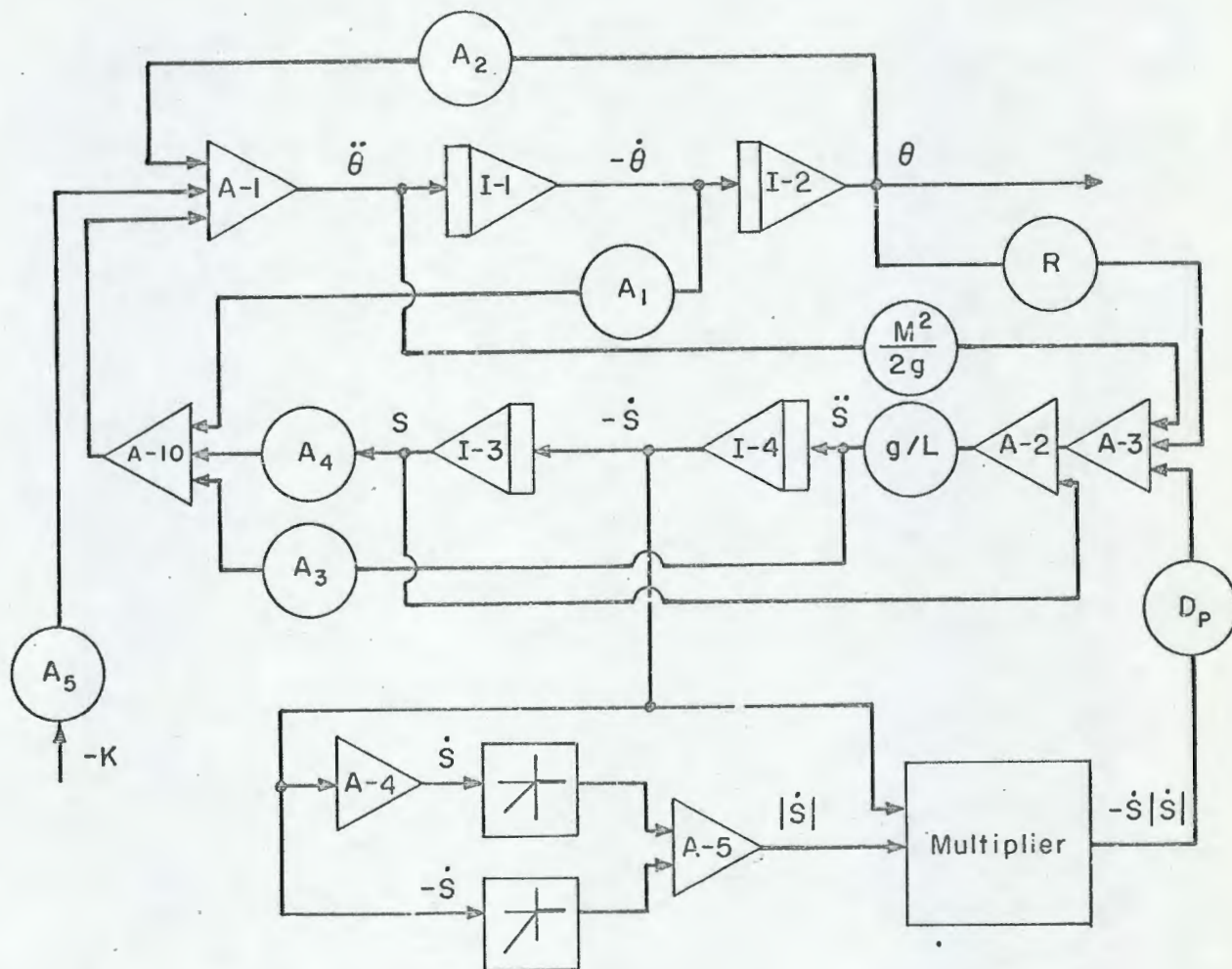


Figure V

Passive System Simulation Diagram

moments applied to the vehicle. Sample results of this simulation are shown in Figures VI through IX. The effect of pipe roughness on tank effectiveness was observed and a sample result is shown in Figure X.

A comparison in effectiveness between the existing DSVR roll-control system and the passive tank stabilizer was made. The roll-loop model reported in reference four was used to simulate the existing system. The responses of this model and the passive tank model are compared in Figure XI for similar disturbance inputs. The variable  $\dot{W}$  in Figure XI is the pumping rate of the list-control pump. This figure illustrates the major deficiency (pump saturation) of the existing system.

#### The Dual Mode System

The simulation of the dual mode system presented some additional problems in that the effect of the valve closure on both the fluid and the vehicle motion must be accounted for. The valve(s) in the cross-connect pipe(s) which is suddenly closed while the fluid is in motion would have the effect of driving  $\dot{S}$  and  $\ddot{S}$  to zero, while  $S$  would remain at the value reached at the time of closure. This assumes an ideal valve which is either fully open or fully closed. In addition, the momentum of the moving fluid column before the valve is closed must be at least partially conserved when the valve is closed. This effect was accounted for by assuming that the angular momentum of the vehicle after the valve closes is equal to the vehicle's angular momentum before the valve closes plus a portion of the angular momentum of the fluid column. This relationship can be shown by the following expression:

$$\dot{\phi}_a = \dot{\phi}_b - k_g k_l \dot{S} \quad 4.4$$

where  $\dot{\phi}_a$ ,  $\dot{\phi}_b$ ,  $k_g$ ,  $k_l$  are the vehicle's angular velocity after the valve closes, the angular velocity before the valve closes, a geometry constant



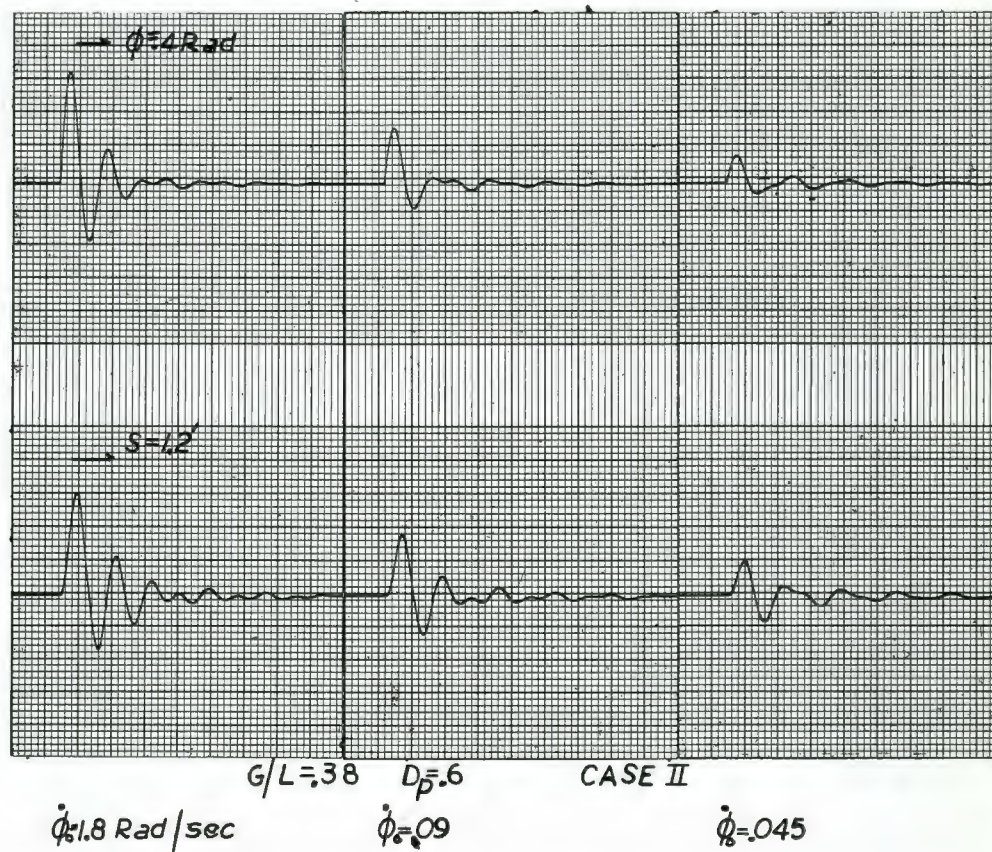
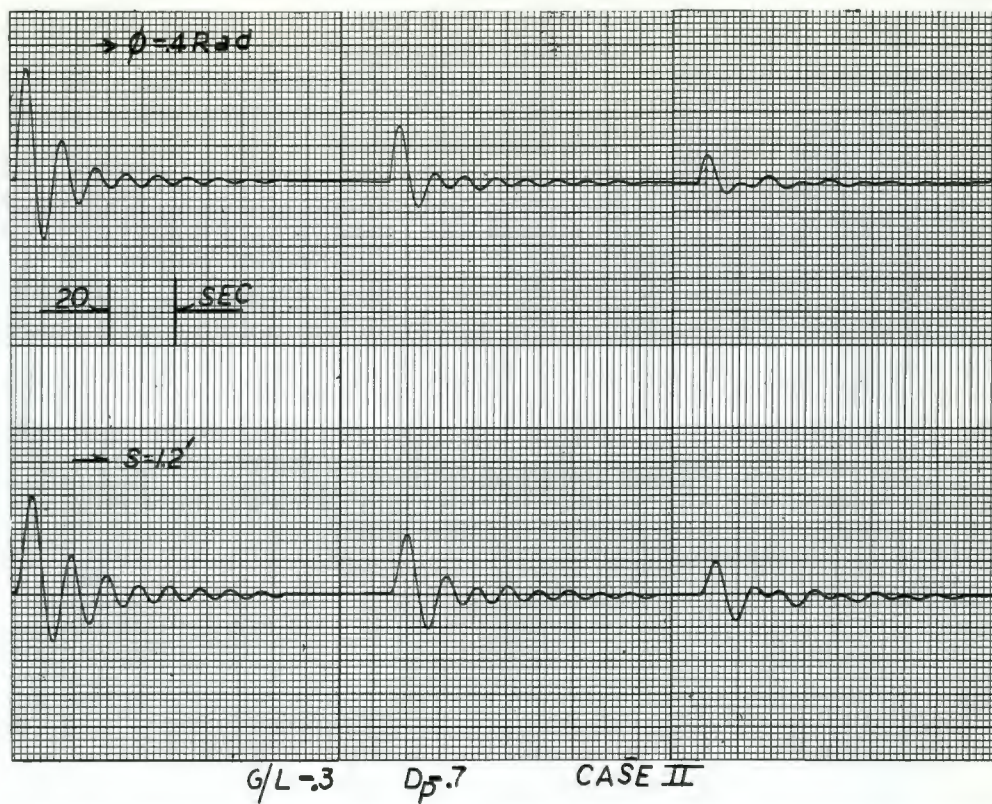
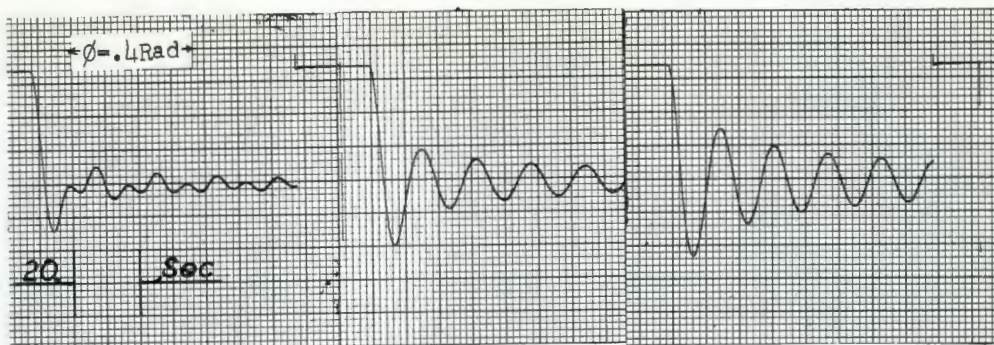
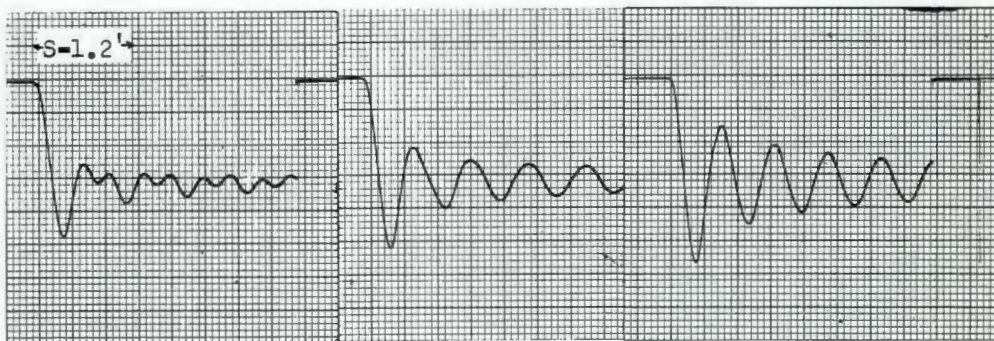


FIGURE VI  
RESPONSES TO INITIAL VELOCITIES



CASE I  $\phi_0 = .34 \text{ Rad}$ 

$$\frac{g}{L} = .30$$

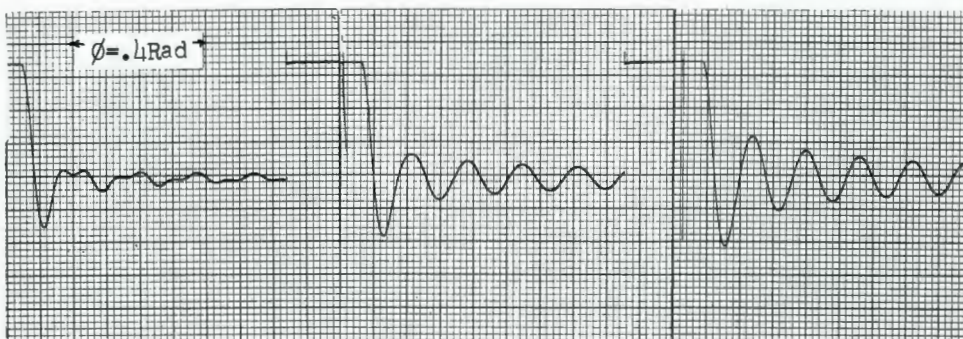
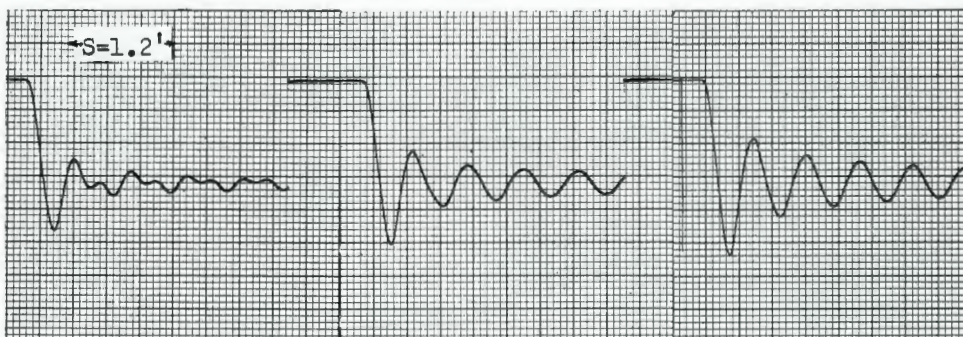
$$D_p = .80$$

$$\frac{g}{L} = .50$$

$$D_p = .40$$

$$\frac{g}{L} = .80$$

$$D_p = .25$$

CASE II  $\phi_0 = .34 \text{ Rad}$ 

$$\frac{g}{L} = .40$$

$$D_p = .70$$

$$\frac{g}{L} = .60$$

$$D_p = .40$$

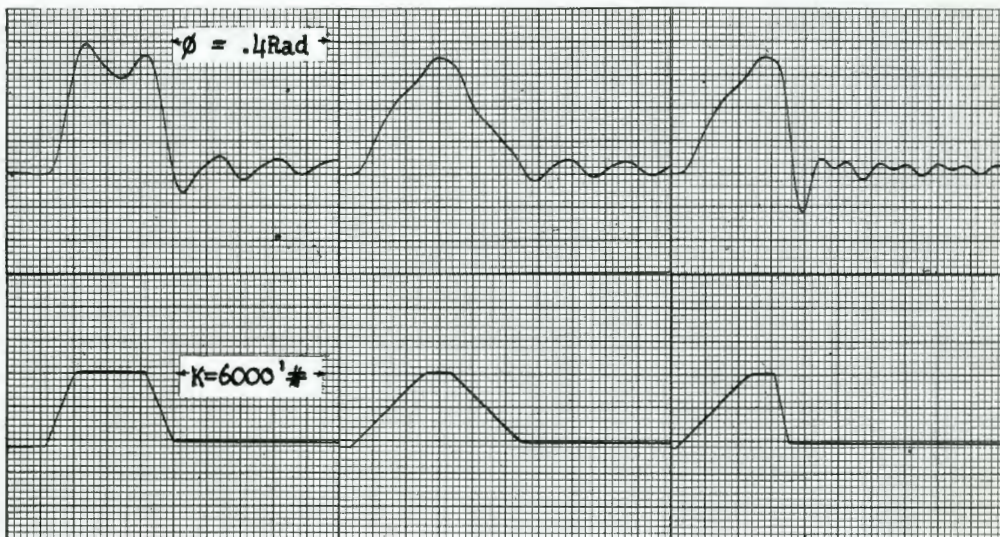
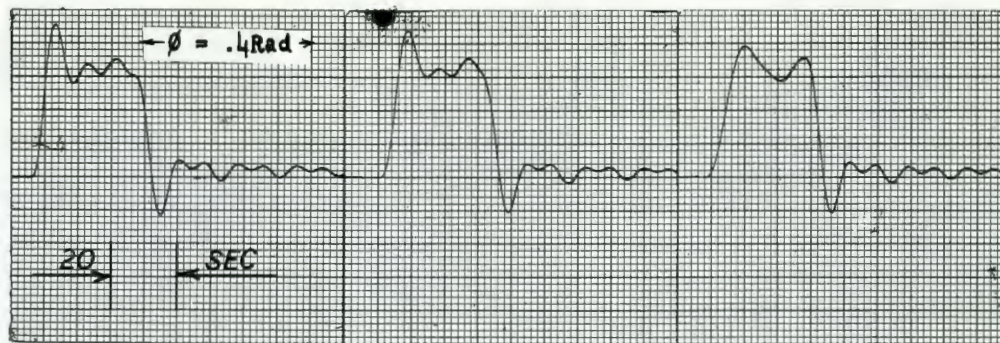
$$\frac{g}{L} = .80$$

$$D_p = .20$$

FIGURE VII

Case I and case II responses to initial heel angle.



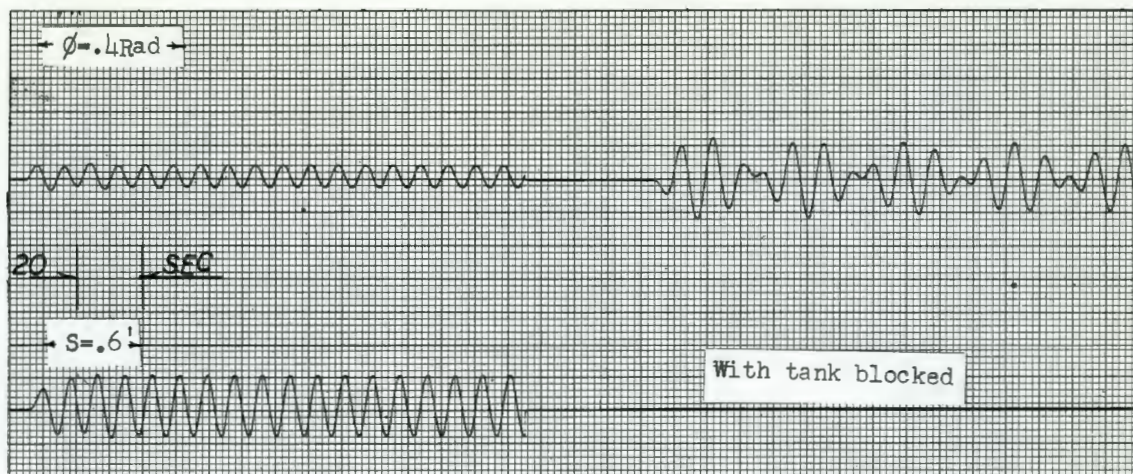


$$g/L = .32 \quad D_p = .65$$

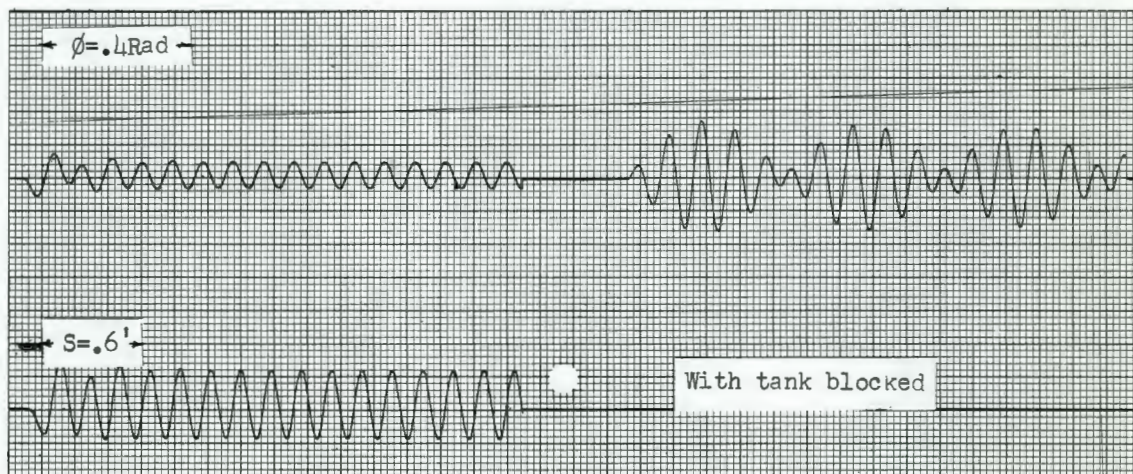
Figure VIII

Case II Responses to Ramp Moments.

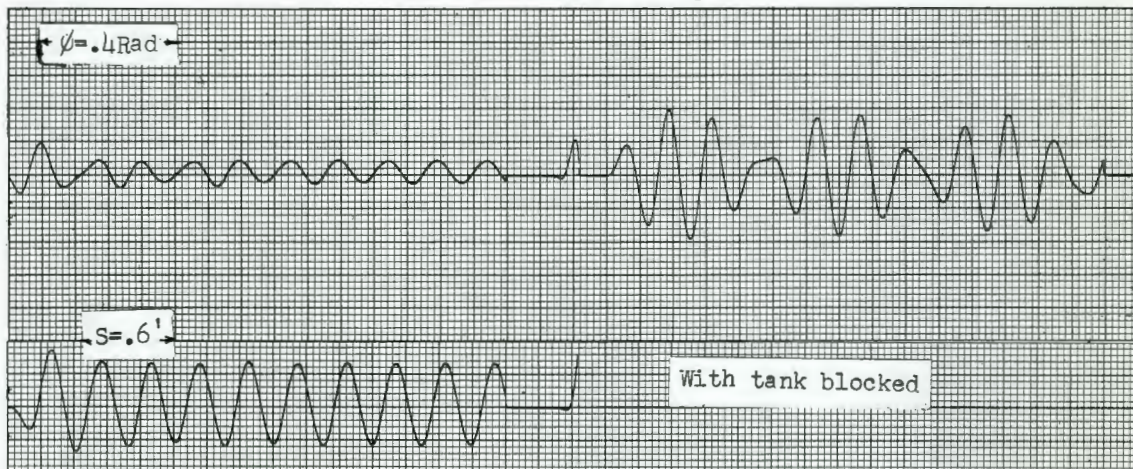




$$f = .123 \text{ cps} \quad g/L = .6 \quad D_p = .3$$



$$f = .110 \text{ cps} \quad g/L = .5 \quad D_p = .35$$



$$f = .071 \text{ cps} \quad g/L = .2 \quad D_p = .6$$

FIGURE IX

Response to periodic disturbances.



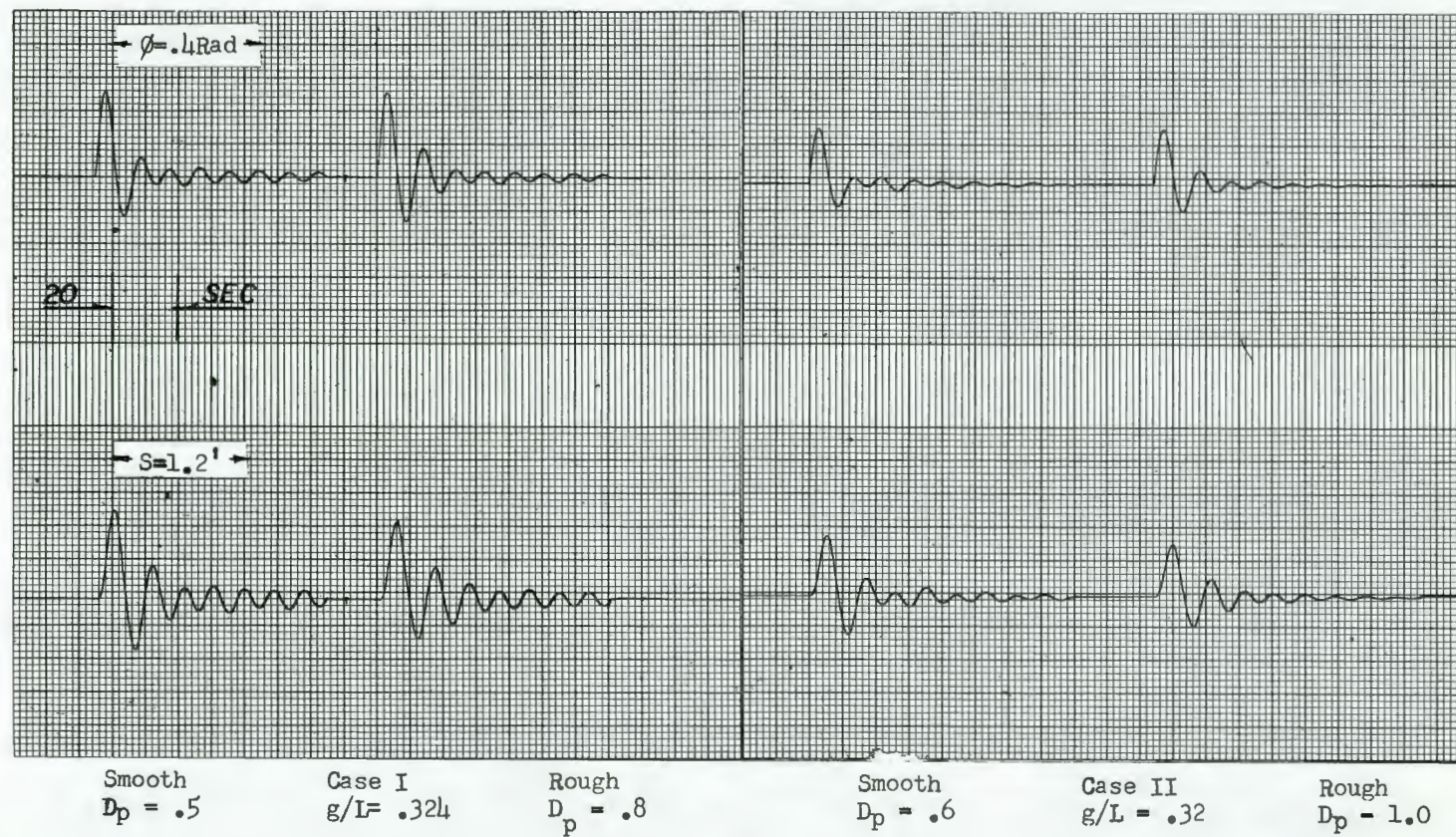


FIGURE X  
Effect of pipe roughness.



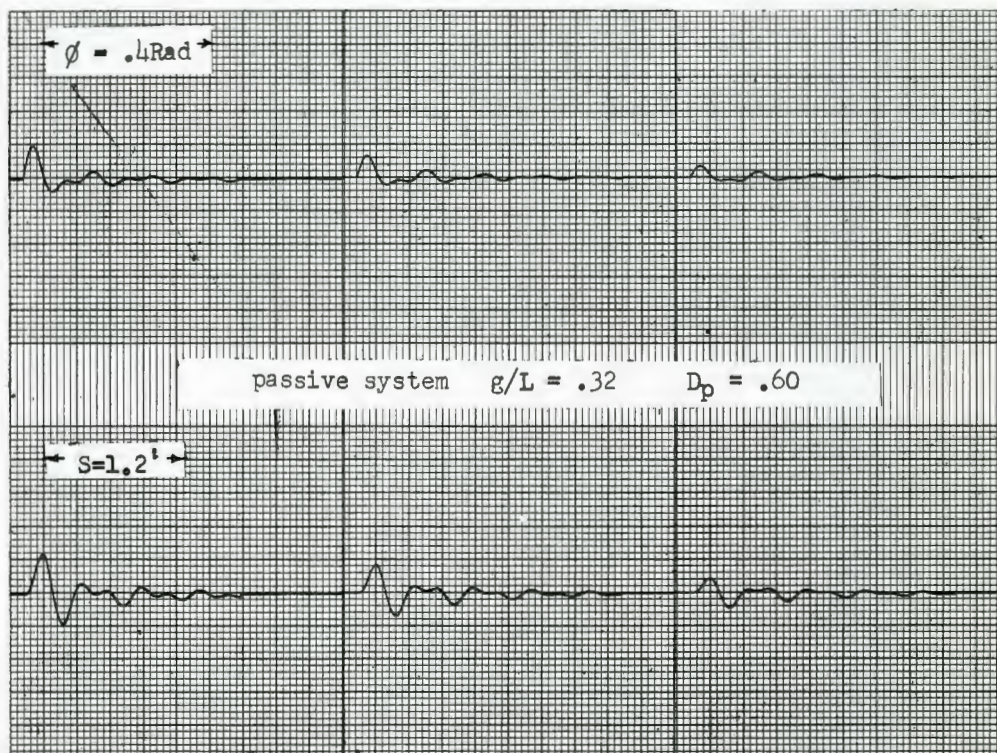
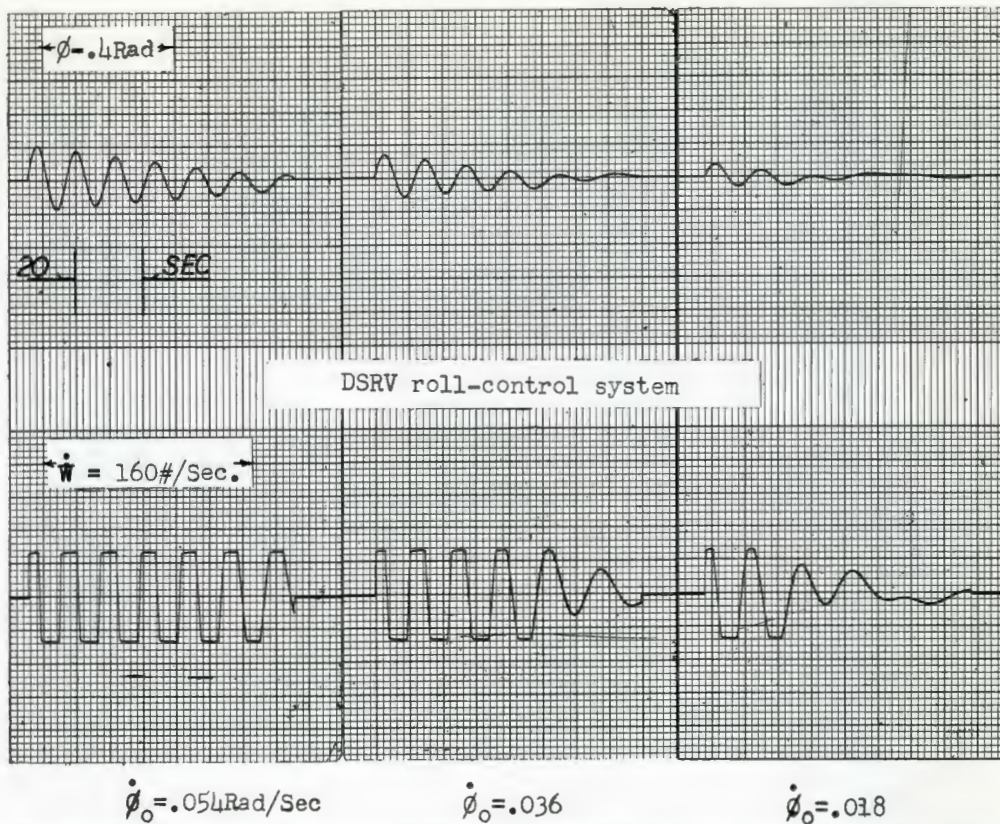


FIGURE XI

Comparison between existing system and the passive system.



relating  $\dot{S}$  to angular momentum, and a variable ( $0 \leq k_1 \leq 1$ ) which will reflect the amount of fluid momentum transferred to the vehicle. A simulation diagram for the valve action is shown in Figure XII.

Operation of the circuit shown in Figure XII depends upon two basic characteristics of the 200T computer.<sup>8</sup> When no mode control is applied to an integrator, it will act as a summing junction for the signals applied to the initial condition inputs. Thus, when the valve is open, the output of I-5 is  $-\dot{\phi} + k_g k_1 \dot{S}$ . When the valve is closed, I-5 becomes an integrator and the output includes the effect of the momentum impulse  $k_g k_1 \dot{S}$ . In the S- channel, when the valve is closed the switches change position and mode control is removed from I-4. Because the disconnected output terminals of the 200T switch units are grounded, this drives  $\dot{S}$  and  $\ddot{S}$  to zero. It also resets I-4 so that when the valve is reopened, S starts from zero. By grounding the input to I-3 when the valve is closed, this integrator goes into a hold mode and the S value present when the closure occurs is retained until the valve reopens.

The dual mode condition was simulated by making step changes in the parameters  $g/L$ ,  $D_p$  and  $k_1$ . The system was assumed initially to be in mode I, which has a short period (large  $g/L$ ). This would facilitate a large mass-transfer rate when the vehicle was initially subjected to a large disturbing moment. At a later time, the tank system is switched to mode II, which is tuned to the natural frequency of the vehicle. The effect of switching modes is similar to complete closure of the cross-connect pipes, but not as severe, because the fluid column would not be completely blocked. In a physical system, mode switching could be accomplished by



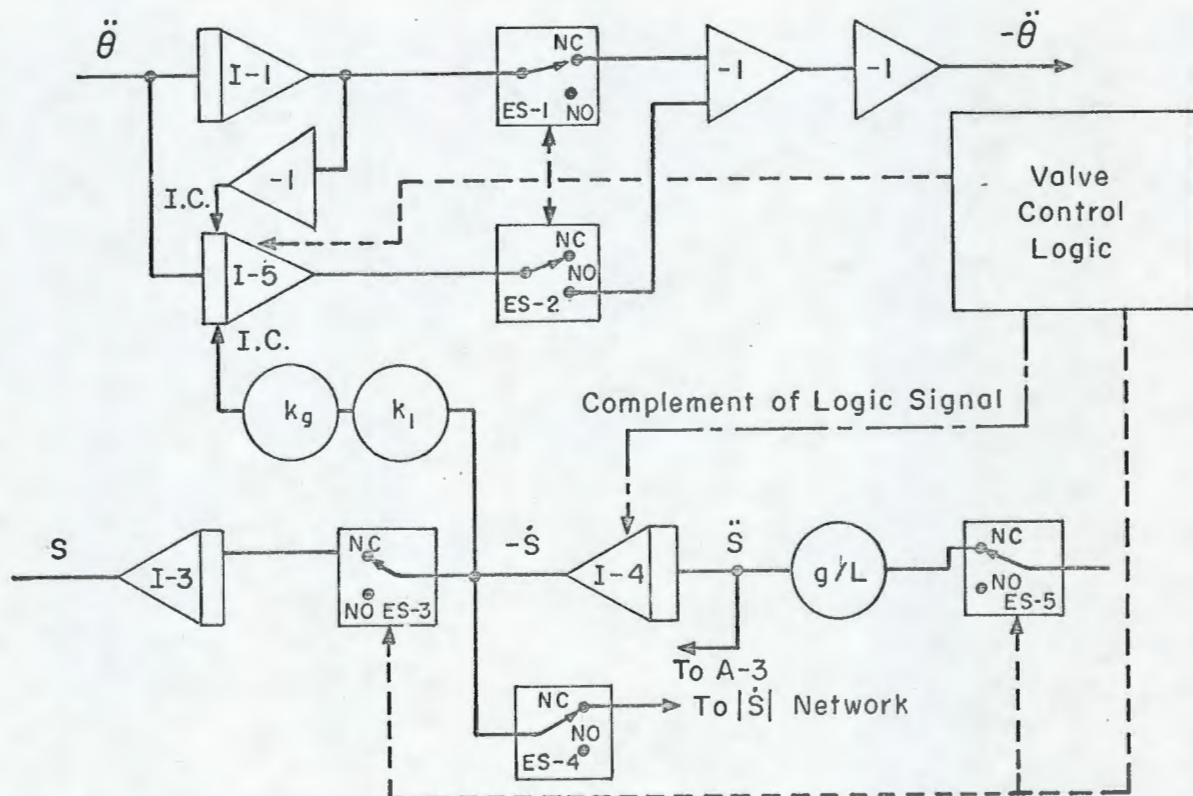


Figure XII

### Valve Simulation Diagram

closure of some of the pipes in a multiple-pipe cross-connect arrangement, or simply by throttling the valve(s) in the system. Figure XIII shows a typical mode-control switching circuit. Note that A-6 and A-7 are required because the electronic switch must be driven by a low impedance source.

The selection of the valve timing and the mode switching criteria was approached on a trial and error basis. Eventually, a very simple switching law was chosen which proved to give satisfactory results. The law is illustrated in Figure XIV. The system responses for sample initial disturbances and mode tunings are shown in Figures XV, XVI and XVII. Figure XVIII illustrates the effect of  $k_1$ .



CHAPTER V

## DISCUSSION OF RESULTS AND CONCLUSIONS

The Passive System

The results of the simulation of the passive system make two very clear points. The effect of tank tuning on roll-stabilization is most obvious. In those cases where the vehicle is subjected to transient disturbances, the most effective stabilization occurs when the tank is tuned to the natural frequency of the vehicle. For a periodic forcing function, the tank must be tuned to the frequency of the disturbance.

The second point revealed by the basic simulation is that fluid transfer rates of 100 - 200 pounds per second are possible in the passive system. (Recall that the maximum pumping rate for the existing DSRV list-control system is only 56 pounds per second.) Observe, for example, in Fig. VI, for the initial velocity disturbance of 0.18 radians per second, the maximum fluid excursion is about 1.32 feet over a time interval of about seven seconds. On the average, this is 96 pounds per second. Note that this example is for a tank tuned slightly below the vehicle natural frequency. When the tank is detuned to a higher frequency, the flow rate is increased.

The comparisons shown in Fig. XI indicate the increased effectiveness gained by using the passive system in lieu of the existing activated system. Fig. XI indicates that pump saturation occurs even with relatively small disturbances. However, this sample result also indicates that the effectiveness of the passive system is relatively independent of the magnitude of the disturbance.



An interesting point is illustrated in Fig. X. Observe that, for the same conditions of tuning the smooth pipe system is more effective in stabilizing the disturbance than is the rough pipe system. This would indicate that there is an optimum value of flow losses which would result in maximum damping effect. This conclusion is reached because, if the system were lossless, there would be no energy dissipated, and therefore no damping effect. If the pipe were infinitely rough, there would be no fluid motion and again no damping effect. Therefore there must be an optimum value between these two end points.

#### The Dual Mode System

The effectiveness of the dual mode system is illustrated in Figs. XV through XVIII. In general, the amount of increased roll reduction from the dual mode operation versus the simple passive system is not large. One could question whether the increased system complexity required for a dual mode system could be justified in terms of the net gains in overall stabilization. Furthermore, the results shown here are the responses to some rather idealized, transient disturbances.

Nevertheless, there are some significant results of this study of a dual mode system. The responses shown in Figs. XV, XVI and XVII indicate that increasing the mode I frequency increases the system's damping. These results also indicate that the mode I frequency should be at least three times larger than the vehicle natural frequency, if significant gains in effectiveness are to be achieved.

Further study of the results of the dual mode operation reveals that the valve action increases the phase difference between the fluid motion

and the vehicle motion. For example, in Fig. XVI, observe that the time between the peak positive value of  $\phi$  and the maximum negative excursion of  $S$  is about nine seconds for the dual mode system, and less than seven seconds for the same sequence in either mode I or mode II alone. Increased phase difference is the principal result achieved from an activated anti-roll system. The point is that the power required to operate a valve would be considerably less than that required by a pump.

### Conclusions

The major conclusion to be drawn from this investigation is that the amount of roll stabilization of the DSRV could be significantly increased through the use of a passive tank system. Under conditions of moderate disturbances, fluid transfer rates well in excess of 100 pounds per second are possible for reasonable tank configurations. It has been shown that a tuned passive system is more effective in stabilizing moderate transient disturbances than is the existing system which is subject to pump saturation. In addition, it has been shown that there is a slight increase in system transient damping when a dual mode passive system is used instead of the simple passive system. The benefit of the dual mode system apparently results from the increased phase difference between the fluid and the vehicle motion.

### Suggestions for Further Investigation

It is recognized that the existing DSRV roll-control system was designed to meet attitude control criteria as well as to stabilize the vehicle in roll. Furthermore, it is realized that any proposals for increasing the



roll stabilization of the DSRV must account for the capability to hover at any angle of heel less than  $45^\circ$  in magnitude. A possible candidate system which employs a passive tank stabilizer and still meets the heel angle requirements would be a passive tank system mounted on a subassembly capable of being rotated about the vehicle's longitudinal axis. The current list-control system could be retained for attitude generation and fine control, or the rotating subassembly could be weighted in such a manner as to produce the required moment when rotated.

In reference to the use of a dual mode system, further study is required to determine if the performance of a passive system subjected to the disturbances of an irregular sea could be improved through dual mode operation.

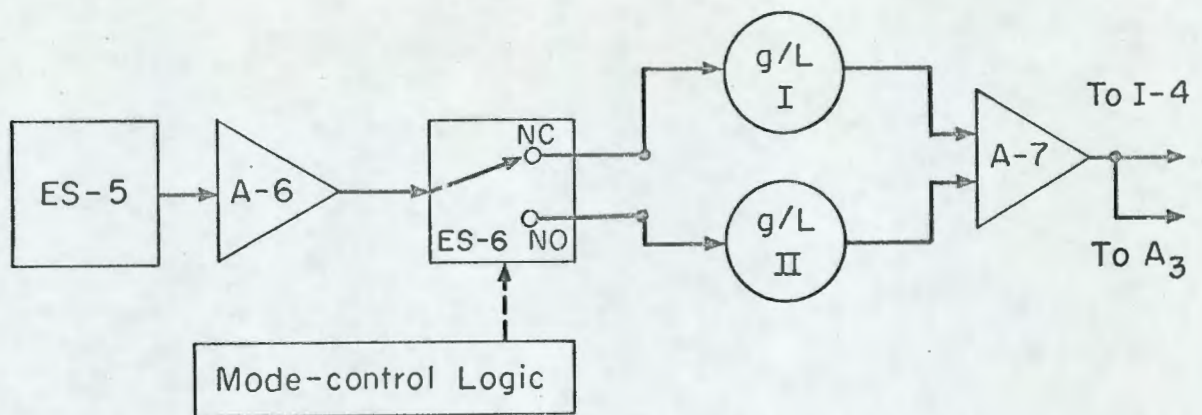


Figure XIII

### Mode Switching Arrangement

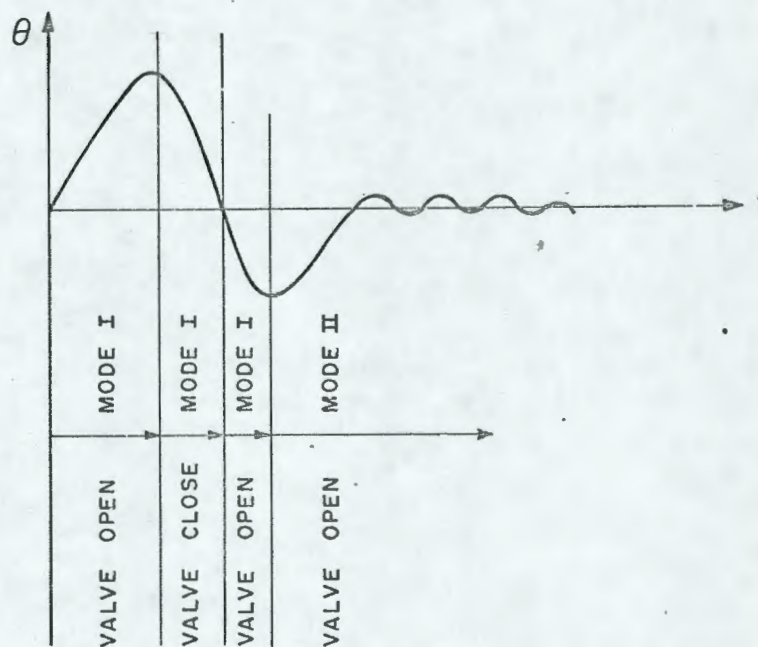


Figure XIV

### Valve Timing and Mode Control



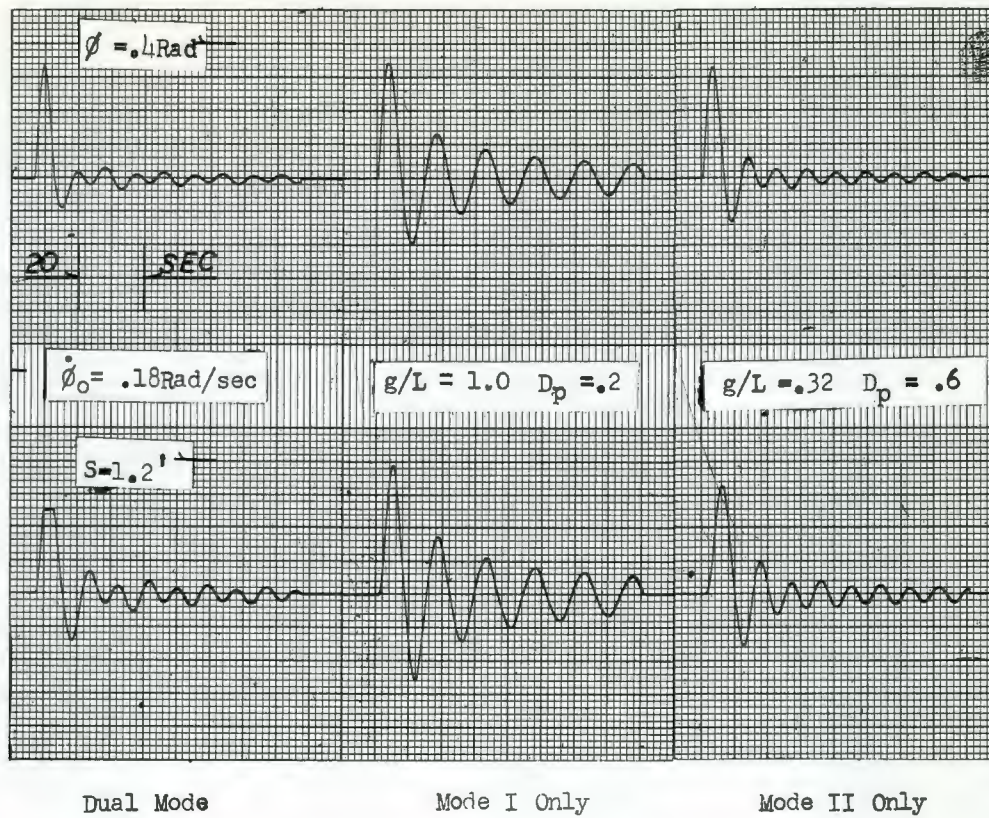


FIGURE XV

Comparison between dual and single mode operation



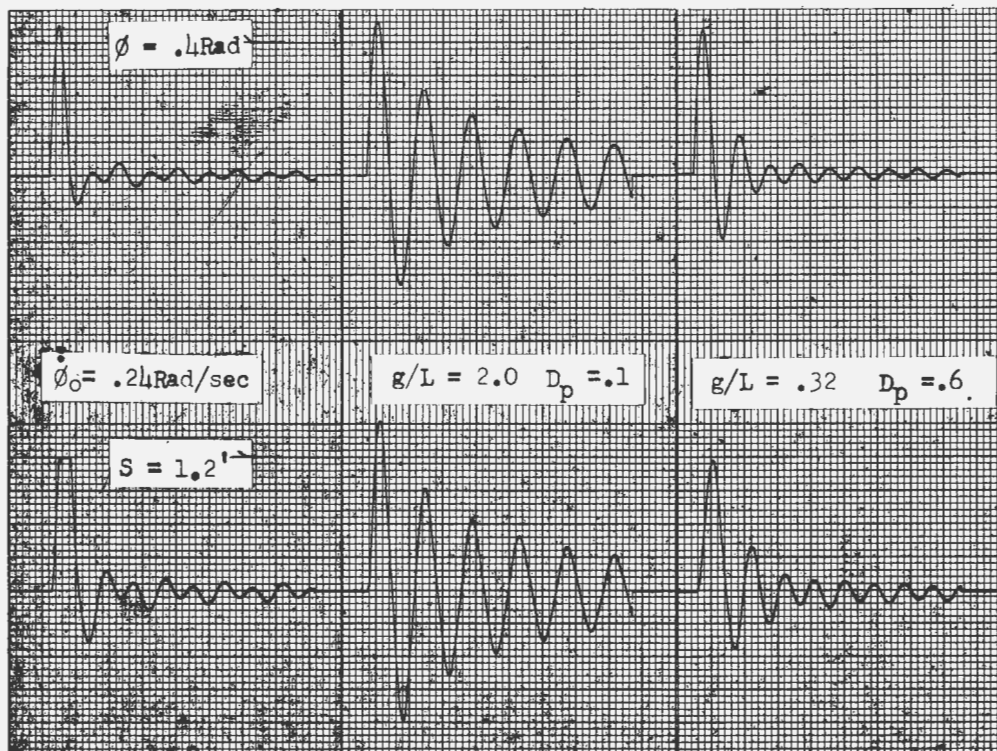
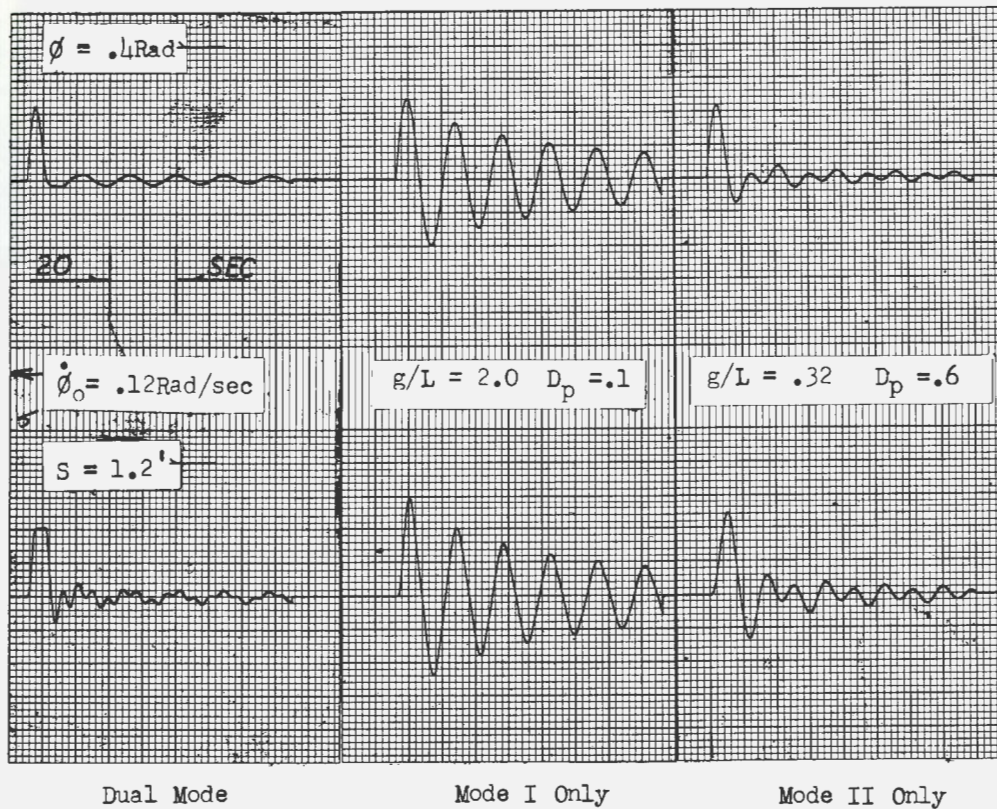


FIGURE XVI

Comparison between dual and single mode operation



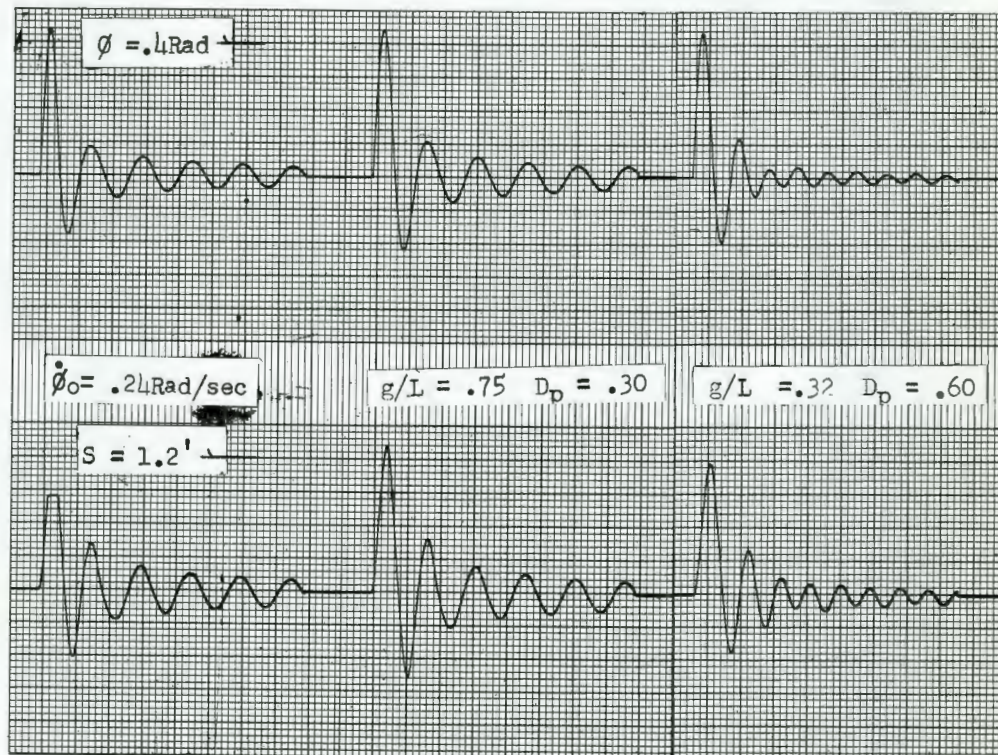
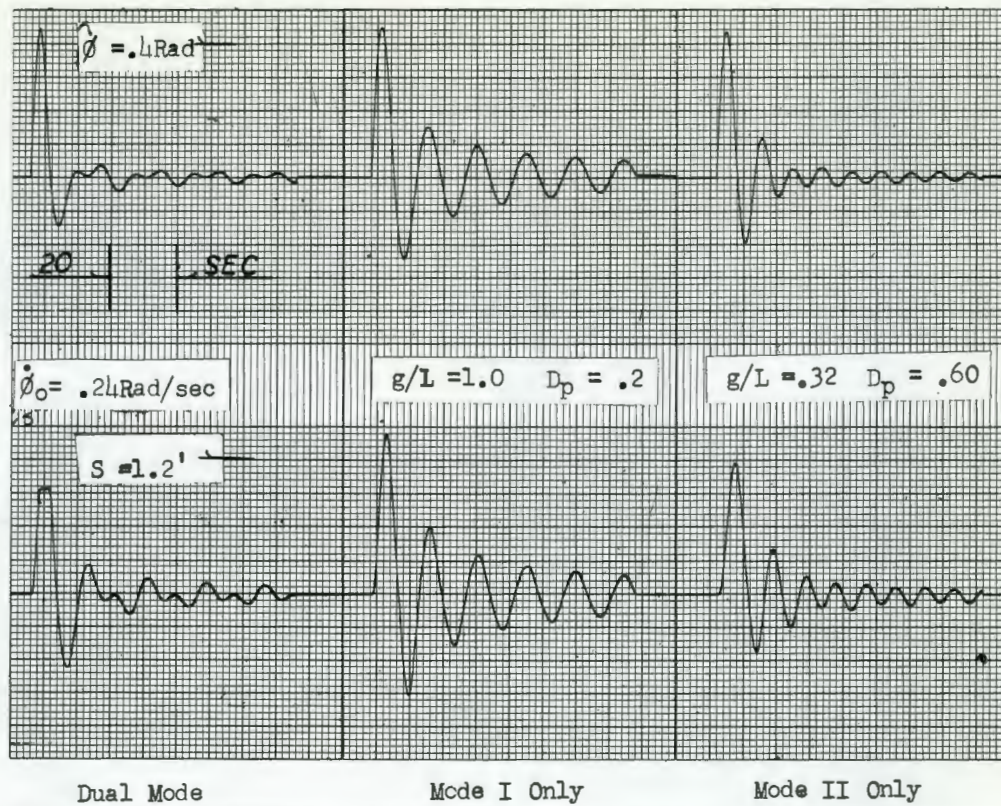


FIGURE XVII

Comparison between dual and single mode operation



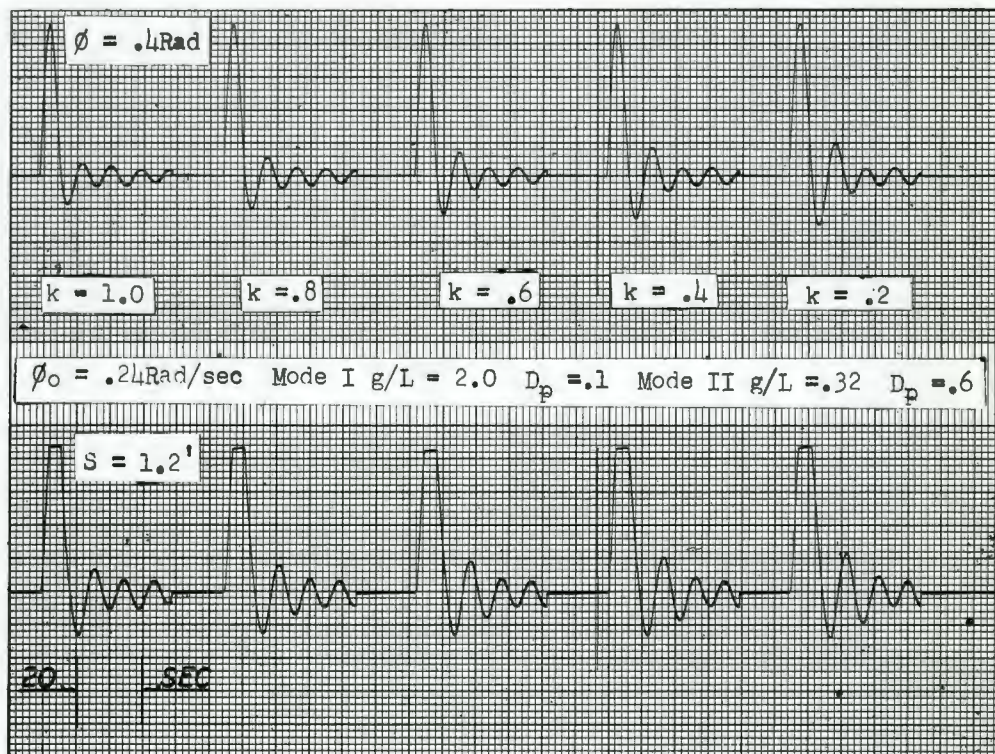


FIGURE XVIII

Dual mode response showing effect of  $k$ .



## APPENDIX I

### THE DSRV MODEL AND PARAMETERS<sup>\*</sup>

Nine generalized coordinates and generalized velocities are sufficient to model the DSRV system. For the vehicle without a moving mass center (no mercury) the velocities  $u$ ,  $v$ ,  $w$ ,  $p$ ,  $q$  and  $r$  describe the vehicle motion. The six needed Lagrange equations are:

$$\frac{d}{dt} \frac{\partial T_v}{\partial u} - r \frac{\partial T_v}{\partial v} + q \frac{\partial T_v}{\partial w} = X \quad \text{I-1}$$

$$\frac{d}{dt} \frac{\partial T_v}{\partial v} - p \frac{\partial T_v}{\partial w} + r \frac{\partial T_v}{\partial u} = Y \quad \text{I-2}$$

$$\frac{d}{dt} \frac{\partial T_v}{\partial w} - q \frac{\partial T_v}{\partial u} + p \frac{\partial T_v}{\partial v} = Z \quad \text{I-3}$$

$$\frac{d}{dt} \frac{\partial T_v}{\partial p} - w \frac{\partial T_v}{\partial v} + v \frac{\partial T_v}{\partial w} - r \frac{\partial T_v}{\partial q} + q \frac{\partial T_v}{\partial r} = K \quad \text{I-4}$$

$$\frac{d}{dt} \frac{\partial T_v}{\partial q} - u \frac{\partial T_v}{\partial w} + w \frac{\partial T_v}{\partial u} - p \frac{\partial T_v}{\partial r} + r \frac{\partial T_v}{\partial p} = M \quad \text{I-5}$$

$$\frac{d}{dt} \frac{\partial T_v}{\partial r} - v \frac{\partial T_v}{\partial u} + u \frac{\partial T_v}{\partial v} - q \frac{\partial T_v}{\partial p} + p \frac{\partial T_v}{\partial q} = N \quad \text{I-6}$$

---

<sup>\*</sup>The material in this Appendix has been drawn from reference 4, and is included here for information only.

$T_v$  is the total vehicle kinetic energy and  $x, y, z, K, M$ , and  $N$  are the forces and moments acting on the vehicle.

Three additional equations are needed to describe the effect of mercury motion. It was assumed that these equations could be reduced to quasi-steady equations defining the center of gravity location from the integrals of the various pumping rates.

The vehicle kinetic energy is given by:

$$T_v = \frac{M}{2} V_G^2 + \frac{1}{2} \bar{w} \int_G w \quad I-7$$

where  $M, V_G, \bar{w}$  and  $\int_G$  are the vehicle mass, the center of gravity velocity, the angular velocity vector about the body axes, and the inertial tensor about the center of gravity. By defining axes  $x', y', z'$  parallel to the body axis and through the center of gravity,

$$\int_G = \begin{bmatrix} I_{x'x'} & I_{x'y'} & I_{x'z'} \\ I_{y'x'} & I_{y'y'} & I_{y'z'} \\ I_{z'x'} & I_{z'y'} & I_{z'z'} \end{bmatrix} \quad I-8$$

The components of the velocity vector  $\bar{V}_G$  are:

$$\bar{V}_G = [u + qz_G - ry_G + \dot{x}_G, v + rx_G - pz_G + \dot{y}_G, w + py_G - qx_G + \dot{z}_G] \quad I-9$$

The inertial tensor about the center of gravity may be related to the inertial tensor  $\int_B^G$  about the center of buoyancy by the parallel axis theorem. For example

$$I_{xx} = I_{x'x'} + M(y_G^2 + z_G^2) \quad I-10$$

By modifying Equation I-8 through the use of a set of equations similar to



I-10 and using I-9, the expression for  $T_v$  (Eq. I-7) may be solved. Substituting this result into Equations I-1 through I-6 yields the full set of dynamical equations for the DSRV. From Equation I-4, the results for the roll mode are:

$$\begin{aligned}
 K = & I_{xx} \dot{p} + I_{xy} (\dot{q} - pr) + I_{xz} (\dot{r} + pq) + I_{yz} (q^2 - r^2) + (I_{zz} - I_{yy})qr \\
 & - Mz_G (\dot{v} - pw + ru + r\dot{x}_G + \ddot{y}_G) + My_G (\dot{w} + pv - qu - q\dot{x}_G + \ddot{z}_G) \\
 & + \dot{I}_{xx} p + \dot{I}_{xy} + \dot{I}_{xz} r + Mx_G (\dot{z}_G r + \dot{y}_G q)
 \end{aligned} \quad I-11$$

Equation I-11 was simplified by making the following assumptions:

- a) Because of xz plane symmetry,  $I_{xy} = I_{yx} = I_{yz} = I_{zy} = 0$
- b) Assume almost fore-aft symmetry in weight distribution

$$I_{xz} = I_{zx} = 0$$

- c) Neglect velocity and acceleration terms of the center of

$$\text{gravity: } \dot{x}_G = \dot{y}_G = \dot{z}_G = \ddot{x}_G = \ddot{y}_G = \ddot{z}_G = 0$$

Note that because of this assumption,  $\dot{I}_{xx} = \dot{I}_{yy} = \dot{I}_{zz} = 0$ .

As a result of the simplifying assumption, Equation I-11 becomes:

$$I_{xx} \dot{p} + (I_{zz} - I_{yy})qr - Mz_G (\dot{v} - pw + ru) + My_G (\dot{w} + pv - pu) = K \quad I-12$$

The forcing term in the above equation has components which are induced because of gravity, hydrodynamic and propulsion effects.

$$K = K_G + K_H + K_p \quad I-13$$

$$\text{The gravity term is: } K_G = (y_G \cos \theta \cos \phi - z_G \sin \phi)w \quad I-14$$

The hydrodynamic term is:

$$\begin{aligned}
 K_H = & K_{\dot{p}}\dot{p} + K_{\dot{v}}\dot{v} + K_{qr}qr + K_{rw}rw + K_{vq}vq + K_{pw}pw \\
 & + K_{v|w|}v|w| + K_{v|u|}v|u| + K_{v|v|}v|v| + K_{p|u|}p|u| \\
 & + K_{r|u|}r|u| + K_{p|p|}p|p| + K_{\text{dist}}
 \end{aligned}
 \tag{I-15}$$

The coefficients of this expression have been determined by model tests in a towing tank.

Propulsion effects result from propeller action, effector action and movement of mercury within the vehicle. For the time being, these effects will remain lumped under the term  $K_p$ .

By combining Equations I-12 through I-15 the general equation describing the vehicle in roll may be obtained. In order to simplify the resulting equation, the relative magnitude of each term was determined by subjecting the system to the following set of standard conditions, and discarding the less important terms. The standard conditions are:

$$\begin{aligned}
 u = v = w &= 1.0 \text{ ft/sec} \\
 \dot{u} = \dot{v} = \dot{w} &= .1 \text{ ft/sec} \\
 p = q = r &= .01 \text{ Rad/sec} \\
 \dot{p} = \dot{q} = \dot{r} &= .01 \text{ Rad/sec} \\
 \phi = \theta = \psi &= .10 \text{ Radians}
 \end{aligned}$$

The roll equation which results is:

$$(I_{xx} - K_p)\dot{p} = (Mz_G + K_v)\dot{v} + K_{v|u|}v|u| + K_{v|w|}v|w| - Mgz_G \sin\phi + K_p \tag{I-16}$$

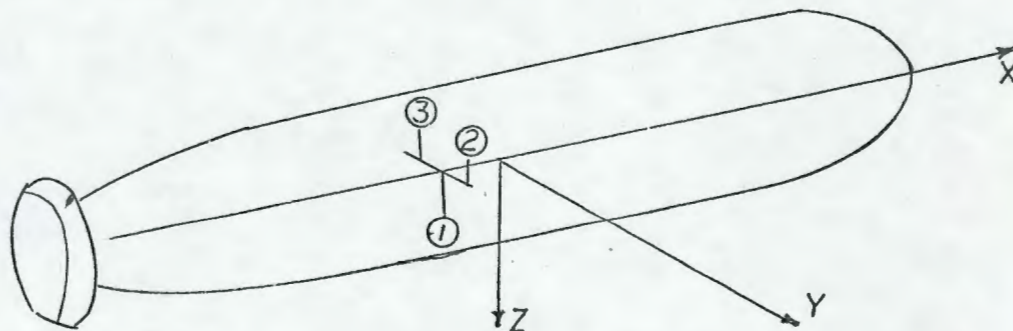
When the cross-coupling between  $u$  and  $p$  is considered, and if the assumption of small roll angles ( $\sin\phi \approx \phi$ ) is made, the basic equation describing



vehicle roll is:

$$(I_{xx} - K_p) \ddot{\phi} = K_{p|u|} |\dot{u}| \dot{\phi} - Mg z_G \ddot{\phi} + K_S \quad I-17$$

where  $K_S$  includes any moment about the x- axis applied to the vehicle.



Tank Arrangement and Coordinate System

Tank	Coordinates			Pump To
	x	y	z	
T-1	- 3.425	0	3.10	T-2, T-3
T-2	- 3.425	2.21	- 2.24	T-3, T-1
T-3	- 3.425	-2.21	- 2.24	T-1, T-2

Total mercury mass 82.5 slugs

Vehicle constants of interest:

$$M = 4363 \text{ slugs}$$

$$z_G = 0.1335 \text{ ft.}$$

$$I_x = 56,200 \text{ slugs-Ft}^2$$

$$K_p = - 5,300 \text{ slugs-Ft}^2$$

$$K_v = 947 \text{ slugs-Ft.}$$

$$K_{v|u|} = 360 \text{ slugs (forward)}$$

$$K_{v|w|} = 687 \text{ slugs}$$

$$K_{p|u|} = - 2,000 \text{ slugs-ft.}$$

Pumping rate ( $\dot{w}$ ) is related to commanded rate by:

$$.083 \frac{dw}{dt} + \dot{w} = \dot{w}_c$$

Maximum pumping rate is 56.2#/Sec.

## APPENDIX II

PARAMETER CALCULATIONS

The calculations illustrated in this section are based on the tank geometry shown in Figure two. The side tank area is assumed to be 0.6 square feet, and the density of mercury is assumed to be 26.3 slugs per cubic foot.

The tank moment is calculated from Equation 2.6:

$$M_{Ty} = \int A(S)r \sin \beta ds.$$

Inspection of Figure one indicates  $ds = r d\beta$ .

Therefore:

$$M_{Ty} = 2 \int_0^{\pi/2} A(S)r^2 \sin \beta d\beta$$

$$M_{Ty} = 2 \int_0^{.453} .6 R^2 \sin \beta d\beta + n \int_{.453}^{\pi/2} A_p r^2 \sin \beta d\beta$$

For case I,  $r = 3.435$  ft.  $R = 3.06$

$$M_{Ty} = 2 \{ .562 + n A_p 3.40 \} \text{ ft}^4 \quad \text{II-1}$$

For Case II, the similar equation is:

$$M_{Ty} = 2 \{ .562 + n A_p 3.68 \} \text{ ft}^4 \quad \text{II-2}$$

The solutions of Equations II-1 and II-2 are tabulated in Table I.

The value of the tank effective length is calculated from Equation 2.9:

$$L = \frac{1}{2} \int \frac{A_T}{A(S)} ds$$



N	$A_p = .00503 \text{ ft}^2$		.00637		.00785		.00955		.0113		.0133	
	Case I	Case II	I	II	I	II	I	II	I	II	I	II
1	1.21	1.116	1.23	1.17	1.26	1.18	1.28	1.19	1.31	1.20	1.35	1.22
2	1.29	1.20	1.34	1.22	1.37	1.24	1.44	1.26	1.50	1.29	1.56	1.32
3	1.38	1.24	1.45	1.27	1.52	1.30	1.60	1.33	1.69	1.37	1.78	1.42
4	1.46	1.28	1.55	1.32	1.65	1.36	1.76	1.40	1.88	1.45	2.01	1.52
5	1.55	1.32	1.66	1.37	1.79	1.42	1.92	1.45	2.07	1.53	2.24	1.62
6	1.63	1.36	1.77	1.42	1.90	1.48	2.08	1.52	2.26	1.62	2.45	1.72
7	1.72	1.48	1.88	1.47	2.05	1.54	2.24	1.59	2.45	1.70	2.67	1.82
8	1.80	1.44	1.98	1.52	2.18	1.62	2.40	1.66	2.64	1.78	2.90	1.92

Table I

TANK MOMENT ABOUT PITCH AXIS ( $M_{Ty}$ )

N	$A_p = .00503 \text{ ft}$		.00637		.00785		.00955		.0113		.0133	
	Case I	Case II	I	II	I	II	I	II	I	II	I	II
1	.07	.10	.09	.12	.11	.15	.13	.18	.16	.22	.18	.26
2	.10	.20	.13	.25	.16	.30	.20	.37	.23	.44	.28	.51
3	.21	.29	.26	.37	.31	.45	.39	.55	.46	.64	.54	.75
4	.28	.39	.35	.49	.43	.60	.52	.71	.61	.85	.73	1.0
5	.35	.48	.44	.61	.54	.73	.65	.90	.70	1.04	.90	1.24
6	.41	.58	.52	.72	.63	.87	.79	1.08	.90	1.24	1.07	1.46
7	.48	.67	.61	.85	.75	1.04	.89	1.24	1.04	1.46	1.23	1.70
8	.55	.77	.69	.96	.85	1.15	1.04	1.40	1.19	1.61	1.40	1.90

Table II

TANK FREQUENCY (SQUARED) g/L

This equation may be written for Case I as:

$$L = \int_0^{453} R \, d\beta + \int_{453}^{\pi/2} \frac{A_T}{n A_P} r \, d\beta$$

$$L = \left\{ 1.39 + \frac{2.31}{n A_P} \right\} \text{ ft.} \quad \text{II-3}$$

For Case II, the similar equation becomes:

$$L = \left\{ 1.39 + \frac{1.65}{n A_P} \right\} \text{ ft.} \quad \text{II-4}$$

The results of Equations II-3 and II-4 appear in Table II, in the form of the parameter  $g/L$ .

The tank curvature constant is defined in Equation 2.10

$$M^2 = \int r \cos \gamma \, ds$$

For Case I  $\gamma = 0$   $ds = r d\beta$

$$M^2 = 2 \int_0^{453} R^2 \, d\beta + 2 \int_{453}^{\pi/2} r^2 \, d\beta$$

$$M^2 = 34.8 \text{ ft}^2 \quad \text{Case I} \quad \text{II-5}$$

$$M^2 = 16.0 \text{ ft}^2 \quad \text{Case II} \quad \text{II-6}$$

The tank moment of inertia is defined in Equation 2.11

$$J_T = \rho r^2 A(S) \, ds$$

For Case I.

$$J_T = 2\rho \left\{ \int_0^{453} R^3 A_T \, d\beta + \int_{453}^{\pi/2} r^3 n A_P \, d\beta \right\}$$



$$J_T = \{408 + 3070 n A_p\} \text{ slugs ft}^2$$

II-7

From this equation the range of  $J_T$  is  $423 \leq J_T \leq 931$  for the Case I geometry.

Similarly for Case II:

$$J_T = \{408 + 94.7 n A_p \int r^2 ds\}$$

$$\text{From Figure two, } r = \frac{1.34}{\sin \beta}$$

$$\therefore J_T = \{408 + 680 n A_p\}$$

II-8

And similarly, the range of  $J_T$  is  $412 \leq J_T \leq 472$  for the Case II geometry.

#### Coefficient Evaluation

The coefficient  $A_5$  is determined from Equation 2.25.

$$A_5 = \left( \frac{1}{I'_x - K'_p + J_T} \right)$$

Using the values for  $I'_x$  and  $K'_p$  given in Appendix I, and the results of Equation II-7 and II-8, it is revealed that  $A_5$  is approximately  $1.62 \times 10^{-5}$  (slug-feet<sup>2</sup>)<sup>-1</sup> for both case I and case II geometry.

A similar solution of Equation 2.27, using the maximum and minimum values of  $M_{Ty}$  listed in Table I for both cases, was obtained. The results are:

Case I	$.316 \leq A_2 \leq .332$	$\text{Sec}^{-2}$	II-9
Case II	$.316 \leq A_2 \leq .320$	$\text{Sec}^{-2}$	II=10

The evaluation of  $A_3$  and  $A_4$  are self-evident.

### Sample Damping Calculations

$$\text{Force} = \rho A_p \{1.5 + f(l/D)\} V^2/2$$

Case I  $l_{\max} = 8$  feet Kinematic viscosity of mercury

$D = .13$  feet Assumed to be  $1.3 \times 10^{-6}$  feet<sup>2</sup>/sec<sup>2</sup>

$n = 1.0$

V in ft/sec	$R \times 10^{-6}$	$f(\text{smth})$	$f(\text{r'gh})$	Smooth 1.5 + $f(l/D)$	Rough	Smooth Lbs.F	Rough Lbs. F	Smooth $\alpha$	Rough $\alpha$
1.	0.1	0.0200	0.0440	2.73	4.60	.478	.735	.478	.735
2.	0.2	0.0175	0.0320	2.58	3.47	1.86	2.51	.465	.627
3.	0.3	0.0160	0.0290	2.48	3.29	3.90	5.17	.433	.575
4.	0.4	0.0150	0.0260	2.42	3.1	6.77	8.67	.422	.542
5.	0.5	0.0145	0.0250	2.39	3.04	10.8	13.3	.432	.532
6.	0.6	0.0140	0.0245	2.36	3.00	14.9	18.9	.413	.524
7.	0.7	0.0135	0.0240	2.33	2.97	19.9	25.4	.406	.518
8.	0.8	0.0130	0.0235	2.30	2.95	25.8	33.0	.403	.516
9.	0.9	0.0128	0.0230	2.29	2.91	32.5	41.3	.401	.506
10.	1.0	0.0127	0.0225	2.28	2.88	40.0	50.5	.40	.505
11.	1.1	0.0125	0.0220	2.27	2.85	48.6	61.2	.402	.506
12.	1.2	0.0124	0.0215	2.26	2.82	57.0	71.0	.397	.492
13.	1.3	0.0123	0.0210	2.255	2.79	66.5	85.0	.394	.502
14.	1.4	0.0122	0.0210	2.25	2.79	77.5	95.6	.395	.488
15.	1.5	0.0122	0.0210	2.25	2.79	87.3	108.0	.388	.480
15.	1.6	0.0122	0.0210	2.25	2.79	101.0	124.5	.393	.486
								$\alpha_{\text{ave}}$	
								.414	.533

TABLE III

### Sample Damping Term Calculations

$$K_{Dp} = \frac{\alpha_{\text{ave}}}{n} \left( \frac{A_T}{A_p} \right)^2$$

$$= \frac{845}{n} \quad (\text{smooth pipe})$$

$$= \frac{1085}{n} \quad (\text{rough pipe})$$



The tank damping term is then defined;

$$D_p \triangleq \frac{K_{Dp}}{2\rho g A_T} = \frac{.83}{n} \text{ (smooth pipe)}$$

$$= \frac{1.07}{n} \text{ (rough pipe)}$$

Table III shows the relation between  $D_p$  and  $A_p$  for  $N$  equal 1.

$A_p = .00503 \text{ ft}^2$		.00637		.00785		.00955		.0113		.0133	
Case	Rough Smooth	Rough Smooth	Rough Smooth	Rough Smooth	Rough Smooth	Rough Smooth	Rough Smooth	Rough Smooth	R'gh Sm'th	R'gh Sm'th	R'gh Sm'th
I	3.92	2.68	2.71	1.91	1.85	1.37	1.62	1.20	1.30	.98	1.07 .83
II	3.01	2.23	2.23	1.71	1.74	1.33	1.37	1.07	1.11	.86	.90 .72

Table IV

Tank Damping As a Function of Pipe Area

REFERENCES

1. J. H. Chadwick, "The Anti-Roll Stabilization of Ships by Means of Activated Tanks" (in 4 parts), Division of Engineering Mechanics, Stanford University, Report 15, December 1950-June 1951.
2. J. H. Chadwick, "On the Stabilization of Roll", Trans. SNAME, Vol. 63 1955, pp. 237-280.
3. J. Vasta, A. J. Giddings, A. Taplin and J. J. Stilwell, "Roll Stabilization by Means of Passive Tanks", Trans. SNAME, Vol. 69, 1961, pp. 411-460.
4. C. Broxmeyer, P. O. Dogan, et al, "Deep Submergence Rescue Vehicle Simulation and Ship Control Analysis", Instrumentation Laboratory, Massachusetts Institute of Technology, Report R-570-A, Feb. 1967.
5. "Passive Anti-Roll Tanks", Design Data Sheet, Department of the Navy, DDS-9290-4, September 1, 1962.
6. W. C. Webster, "Analysis of the Control of Activated Anti-Roll Tanks", Paper presented at the Annual SNAME Meeting, New York, New York, November 15-18, 1967.
7. R. H. Sabersky and A. J. Acosta, "Fluid Flow" (text) 1964, The MacMillan Company, New York, N. Y.
8. "200T Analog Computer Operating Manual", Electronic Systems Laboratory, Massachusetts Institute of Technology, February, 1967
9. J. L. Synge and B. A. Griffith, "Principles of Mechanics" (text), 1959, McGraw-Hill Book Company, New York, N. Y.